

# On the energetics of chemolithotrophy in nonequilibrium systems: case studies of geothermal springs in Yellowstone National Park

W. P. INSKEEP, G. G. ACKERMAN, W. P. TAYLOR, M. KOZUBAL, S. KORF AND R. E. MACUR

*Thermal Biology Institute and Department of Land Resources and Environmental Sciences, Montana State University, Bozeman, Montana, USA*

## ABSTRACT

Chemolithotrophic micro-organisms are important primary producers in high-temperature geothermal environments and may catalyse a number of different energetically favourable redox reactions as a primary energy source. Analysis of geochemical constituents followed by chemical speciation and subsequent calculation of reaction free energies ( $\Delta G_{\text{rxn}}$ ) is a useful tool for evaluating the thermodynamic favourability and potential energy available for microbial metabolism. The primary goal of this study was to examine relationships among geochemical gradients and microbial population distribution, and to evaluate the utility of energetic approaches for predicting microbial metabolism from free-energy calculations, utilizing as examples, several geothermal habitats in Yellowstone National Park where thorough geochemical and phylogenetic analyses have been performed. Acidic (pH ~ 3) and near-neutral (pH ~ 6–7) geothermal springs were chosen for their range in geochemical properties. Aqueous and solid phase samples obtained from the source pools and the outflow channels of each spring were characterized for all major chemical constituents using laboratory and field methods to accurately measure the concentrations of predominant oxidized and reduced species. Reaction free energies ( $\Delta G_{\text{rxn}}$ ) for 33 oxidation–reduction reactions potentially important to chemolithotrophic micro-organisms were calculated at relevant spring temperatures after calculating ion activities using an aqueous equilibrium model. Free-energy values exhibit significant variation among sites for reactions with pH dependence. For example, free-energy values for reactions involving  $\text{Fe}^{3+}$  are especially variable across sites due in large part to the pH dependence of  $\text{Fe}^{3+}$  activity, and exhibit changes of up to  $40 \text{ kJ mol}^{-1}$  electron from acidic to near neutral geothermal springs. Many of the detected 16S rRNA gene sequences represent organisms whose metabolisms are consistent with exergonic processes. However, sensitivity analyses demonstrated that reaction free energies do not generally represent the steep gradients in local geochemical conditions resulting from air–water gas exchange and solid phase deposition that are important in defining microbial habitats and 16S rRNA gene sequence distribution within geothermal outflow channels.

Received 3 October 2005; accepted 28 December 2005

Corresponding author: W. P. Inskeep. Tel.: 406-994-5077; fax: 406-994-3933; e-mail: binskeep@montana.edu.

## INTRODUCTION

In many volcanic, hydrothermal and geothermal environments, chemolithoautotrophs represent the primary producers, capable of metabolism on the simplest and among the most common inorganic compounds in the universe (e.g.  $\text{CO}_2$ ,  $\text{H}_2$ ,  $\text{CH}_4$ , S, Fe,  $\text{O}_2$ ). The oxidation–reduction reactions mediated by chemoautotrophic micro-organisms are central to biogeochemical cycling and represent a direct link among adapted microbial populations and geochemical processes (Newman & Banfield,

2002; Reysenbach & Shock, 2002). There has been significant interest in utilizing thermodynamic approaches and energetic calculations to evaluate the favourability and amount of energy potentially available for chemolithotrophic metabolism for numerous electron donor–acceptor combinations (Amend & Shock, 2001; Amend *et al.*, 2003; Shock *et al.*, 2005). Recent efforts include a significant compilation of temperature-dependent standard state Gibbs free-energy values ( $\Delta G_{\text{rxn}}^\circ$ ) for redox couples potentially important for chemotrophic metabolism (Amend & Shock, 2001). Subsequent calculation of actual

free-energy values corresponding to specific environmental conditions (i.e. activities of relevant chemical species) provides a mechanism for determining which reactions are exergonic in a particular environment. Moreover, it is often inferred that the redox couples yielding the greatest amounts of energy will translate to a competitive biological advantage, or that the most thermodynamically favoured reactions are the most important reactions for microbial metabolism (e.g. Spear *et al.*, 2005a).

The thermodynamic favourability of some redox couples will vary among different environments or across geochemical gradients common in soil–water–sediment systems. Consequently, an energetic profile of environmental systems is certainly useful for correlating geochemical energy availability with the distribution of specific, uniquely adapted populations (e.g. Ward *et al.*, 1998), and in customizing appropriate cultivation strategies for specific microbial metabolisms. However, not all exergonic redox couples will necessarily be utilized by micro-organisms in a given environment. Furthermore, the most thermodynamically favoured redox couple may not necessarily correlate with the predominant microbial metabolism in a particular environment (Macur *et al.*, 2004a). While energetic calculations are useful for inventorying the energy available from various redox couples, interpretations regarding predominant microbial metabolisms in dynamic environments should rely on multiple lines of evidence, not solely on the absolute magnitude of free energy available in an exergonic reaction. One of the long-term goals of our research program in geothermal systems is to determine how mass transfer rates, reaction kinetics and microbial specialization have been integrated in time and space. Although exergonic reactions are required for microbial energy yield, it is critical to explore other important factors that determine which of the many exergonic redox reactions are actually used by micro-organisms and why. As a part of this larger goal, the specific objectives of the current study were to (i) examine biogeochemical processes controlling redox cycling in geothermal springs of YNP, (ii) establish the predominant geochemical gradients that occur down gradient of geothermal discharge, (iii) compare observed changes in geochemistry and microbial population distribution with changes in the free-energy distribution among sites and across a suite of redox couples, and (iv) evaluate the utility and sensitivity of energetic approaches for assessing possible variations in microbial metabolism across observed geochemical gradients. The natural systems employed in this study include several geothermal habitats in Yellowstone National Park where thorough geochemical and phylogenetic analyses have been performed.

## METHODS

### Geothermal sites

The sites chosen for this study include geothermal springs located in the One Hundred Springs Plain of Norris Geyser

Basin (NGB), the Rainbow Springs (RS) group and the Joseph's Coat (JC) Springs group of Yellowstone National Park (YNP). The coordinates of the subject springs are as follows: NGB-D (44°43'54.8"N, 110°42'39.9"W), NGB-B (44°43'53.4"N, 110°42'40.9"W), NGB-S (44°43'75.7"N, 110°42'74.7"W), NGB-PS (44°43'36.0"N, 110°42'29.8"W), RS2 (44°45'59.6"N, 110°16'08.2"W) and JC3 (44°44'21.4"N, 110°19'28.2"W). The geothermal springs in Norris Geyser Basin have also been analysed periodically for a full suite of chemical constituents by the US Geological Survey as part of geothermal discharge inventory programs in YNP (Ball *et al.*, 2002). All springs exhibit source water temperatures ranging from 75 to 90 °C and flow rates ranging from approximately 10–50 L min<sup>-1</sup>. During the last 3 years (2003–05), aqueous and solid phase samples have been subjected to detailed chemical characterization and molecular analyses to identify microbial populations (16S rDNA sequence analysis) present as a function of distance from spring discharge. Transects of four to six sampling points originating at the source pool and continuing down-gradient until approximately 50 °C were sampled quarterly for 2 years at NGB-B and NGB-PS (2003–05). Due to the remote locations of Rainbow and Joseph's Coat Springs, transects at RS2 and JC3 were sampled annually for 3 years during the summers of 2003–05.

### Aqueous geochemistry and dissolved gases

Two aqueous samples at each location were filtered (0.2 µm) on site directly into sterile 50 mL screw-cap tubes. One sample was preserved in 0.1 M HNO<sub>3</sub>, then analysed using inductively coupled plasma spectrometry (ICP) for total dissolved Ca, Mg, Na, K, Si, Al, As, Fe and B, and trace elements including Cd, Cr, Cu, Mn, Ni, Pb, Sb, Se and Zn. One sample was left unacidified and analysed for predominant inorganic anions (F<sup>-</sup>, Cl<sup>-</sup>, SO<sub>4</sub><sup>2-</sup>, NO<sub>3</sub><sup>-</sup>, CO<sub>3</sub><sup>2-</sup>, S<sub>2</sub>O<sub>3</sub><sup>2-</sup>, AsO<sub>4</sub><sup>3-</sup>) using ion exchange chromatography (IC) (Dionex Corp. (Sunnyvale, CA, USA) AS16-4 mm column), and aqueous NH<sub>4</sub><sup>+</sup> using the phenolate colourimetric (A<sub>630 nm</sub>) procedure on a flow injection analyser (APHA, 1998). Dissolved inorganic C (DIC) and dissolved organic C (DOC) were determined on separate samples taken in closed headspace serum bottles using a C analyser (Dohrmann DC-80; Teledyne, Mason, OH, USA). In addition, several redox sensitive species were analysed on site including Fe<sup>II</sup> and Fe<sup>III</sup> using the ferrozine method (To *et al.*, 1999) employing a filtered (0.2 µm) sample, and total dissolved sulfide (DS) using the amine sulfuric acid method (APHA, 1998) with unfiltered samples (to avoid rapid degassing of H<sub>2</sub>S(aq) upon filtration). The amount of As<sup>III</sup> and As<sup>V</sup> was determined using atomic absorption spectrometry (hydride generation) on samples untreated and treated with Na borohydride in the field (Langner *et al.*, 2001), where As(III) is then calculated as the difference between arsenate As(V) and total soluble As (As<sub>T8</sub>). Aqueous pH and temperature values were obtained on site using a Mettler-Toledo portable ion meter (MA130) equipped with a temperature

probe, where pH 1.68 and 4.01 buffers were calibrated at spring temperatures.

Dissolved gas species including H<sub>2</sub>, CH<sub>4</sub> and CO<sub>2</sub> were determined using headspace gas chromatography. Closed headspace aqueous geothermal samples were collected using a peristaltic pump with an in-line 0.2 µm filter. After a 4–5 pore-volume purge, 100-mL serum bottles were capped with zero headspace using butyl-acetate stoppers. A known volume of liquid was withdrawn and replaced with an equivalent volume of N<sub>2</sub>(g) and the bottles incubated with intermittent shaking for 60 min. Preliminary analyses determined that an equilibration time of approximately 60 min was required for gas–water partitioning. Samples of the headspace were injected into a portable Varian gas chromatograph (Model CP2900) using Ar and N<sub>2</sub> as carrier gases and analysed for H<sub>2</sub>, CH<sub>4</sub> and CO<sub>2</sub> on a dual-channel thermal conductivity detector system. Values of headspace gas concentrations were then used to calculate original dissolved gas concentrations using temperature-corrected Henry's Law constants for each gas (Amend & Shock, 2001), and a mass balance equation for total dissolved gas prior to headspace equilibration:

$$\text{Henry's Law: } K_{\text{H}} = c(\text{aq})/c(\text{g}) \quad (1)$$

$$\text{Mass balance: } [c(\text{aq})_{\text{sample}} V_{\text{L}}] = [c(\text{g})_{\text{equil}} V_{\text{g,eq}}] + [c(\text{aq})_{\text{equil}} V_{\text{L,eq}}] \quad (2)$$

Where  $K_{\text{H}}$  = Henry's Law constant at temperature of incubation (temperature adjusted values of  $K_{\text{H}}$  determined from thermodynamic constants reported in Amend & Shock, 2001),  $c$  = concentration in either aqueous or gas phases (mol L<sup>-1</sup>), and  $V$  = volume of liquid or gas. Concentrations of dissolved O<sub>2</sub> were determined in the field using the Winkler method (APHA, 1998).

### Solid phase geochemistry

Samples of microbial mats and associated solid phases were subjected to a suite of analytical procedures to determine the composition, structure and mineralogy of solid phases deposited within the outflow channels including: (i) X-ray diffraction (XRD), (ii) scanning electron microscopy and energy dispersive analysis of X-rays (SEM/EDAX), (iii) transmission electron microscopy (TEM) of glutaraldehyde-fixed and epoxy-infiltrated thin sections, (iv) X-ray absorption near edge structure (XANES) spectroscopy, extended X-ray absorption fine structure (EXAFS) spectroscopy using a synchrotron light source at the Stanford Radiation Laboratory (SSRL), and (v) total chemical analysis of mat samples via acid digestion (HNO<sub>3</sub>-HClO<sub>4</sub>-HF at 110 °C). Although it is beyond the scope of this manuscript to report all information on solid phase structure and composition, some data are discussed as they relate to the energetic analyses of these systems.

### Chemical speciation and thermodynamic calculations

Chemolithotrophic thermophiles may derive energy from a wide variety of inorganic electron transfer reactions. Recent literature has outlined details of energetic calculations necessary to evaluate the favourability of redox reactions under specific environmental conditions (Amend & Shock, 2001; Amend *et al.*, 2003). Briefly, the free energies ( $\Delta G_{\text{rxn}}$ , kJ mol<sup>-1</sup>) of 33 potentially important redox couples were calculated using the expression:

$$\Delta G_{\text{rxn}} = \Delta G_{\text{rxn}}^{\circ} + RT \ln(Q_{\text{rxn}}) \quad (3)$$

where  $\Delta G_{\text{rxn}}^{\circ}$  is the standard state free energy of reaction (temperature dependent) and  $Q_{\text{rxn}}$  is the reaction quotient calculated using actual activities of chemical species (Stumm & Morgan, 1996). Temperature-dependent values of  $\Delta G_{\text{rxn}}^{\circ}$  were obtained from Amend & Shock (2001). Values of  $\Delta G_{\text{rxn}}^{\circ}$  not available in the literature were calculated using temperature corrected standard free energies of formation ( $\Delta G_{\text{f}}^{\circ}$ ) (Amend & Shock, 2001). Activities of chemical species were calculated with the aqueous equilibrium model, Visual MINTEQ (Allison *et al.*, 1991), using measured values of total soluble chemical constituents as input values. As discussed in Amend *et al.* (2003), solid phase, gas and redox equilibria were suppressed during chemical speciation calculations to accurately represent the solution as sampled.

### Microbial community analysis: DNA extraction, amplification and sequencing

Microbial mat samples were analysed using molecular methods to assess the distribution of 16S rDNA sequences detectable across different geochemical and temperature gradients observed in the source pools and outflow channels (Jackson *et al.*, 2001; Inskeep *et al.*, 2004; Macur *et al.*, 2004a). Briefly, solid phase microbial mats were sampled using sterile tools and tubes, and immediately placed on dry ice for transport to a –80 °C freezer. Total DNA was extracted from the samples using the FastDNA SPIN Kit for Soil (Q-Biogene, Irvine, CA, USA). Primers for near full-length polymerase chain reaction (PCR) of 16S rRNA genes consisted of the *Bacteria*-specific primer Bac8f (5'-AGAGTTTGATCCTGG-CTCAG-3') and the universal primer Univ1392r (5'-ACGG-GCGGTGTGTAC-3'). The Archaeal domain was targeted using Archaea-specific primer Arc2f (5'-TTCCGGT-TGATC-CYGCCGGA-3') and universal primer Univ1392r. Purified PCR products were cloned using the pGEM-T Vector System from Promega Corp. (Madison, WI) and the inserts were sequenced using T7 and SP6 primers (TGEM, Phoenix, AZ, USA). 16S rDNA diversity and distribution was also examined in several springs using denaturing gradient gel electrophoresis to separate short 16S rDNA fragments (322–461 bp; see Macur *et al.*, 2004a and Inskeep *et al.*,

2004). Resultant sequences were edited and deposited in GenBank (Benson *et al.*, 2005). Although beyond the scope of the current manuscript to discuss all phylogenetic data from these YNP geothermal systems, reference is made to specific 16S rDNA sequences found in these environments using GenBank Accession numbers.

## RESULTS

### Source water geochemistry

The geothermal springs featured in this energetics analysis include acid-sulfate-chloride (ASC) springs of Norris Geyser Basin (pH ~ 3), an acid-sulfate (AS) spring from the Rainbow Spring group (pH ~ 2.6) and two near-neutral springs containing significant levels of total soluble arsenic (Fig. 1). Previous reports have discussed geochemical and 16S rDNA analysis of the two ASC springs from Norris Geyser Basin (NGB-B = Beowulf Spring, Inskeep *et al.*, 2004; NGB-S = Succession Spring; Macur *et al.*, 2004a). The ASC springs of NGB have exhibited tightly constrained  $\text{Cl}^-/\text{SO}_4^{2-}$  ratios of 9–10 over the course of our sampling program since 1999 (Langner *et al.*, 2001; Inskeep *et al.*, 2004; Macur *et al.*, 2004a). The ASC geothermal source waters yield ionic strengths of near 0.016 M, comprised primarily of  $\text{Na}^+$ ,  $\text{H}^+$ ,  $\text{Cl}^-$  and  $\text{SO}_4^{2-}$  (Table 1). More importantly for chemolithotrophic metabolism, the source waters of these springs contain significant quantities of reduced inorganic constituents including  $\text{H}_2$ ,  $\text{H}_2\text{S}$ ,  $\text{Fe}^{\text{II}}$ ,  $\text{As}^{\text{III}}$ ,  $\text{NH}_4$  and  $\text{CH}_4$  (Table 1).

The source waters of Rainbow Spring (RS2) are also acidic (pH 2.6), but otherwise are significantly different from the

ASC springs of Norris Basin (Table 1). Most notably, the dominant anion in RS2 is sulfate rather than chloride, yielding  $\text{Cl}^-/\text{SO}_4^{2-}$  ratios of ~0.02 consistently over 3 years of sampling (2003–05). Furthermore, total soluble concentrations of  $\text{NH}_4^+$  and  $\text{Fe}^{2+}$  are fairly high at 1.7 mM and 100  $\mu\text{M}$ , respectively. The source waters contain significant quantities of dissolved  $\text{H}_2$ ,  $\text{CH}_4$  and  $\text{CO}_2$ ; however, total soluble sulfide has not exceeded 10  $\mu\text{M}$  and total soluble As levels are low relative to many YNP geothermal springs (Stauffer & Thompson, 1984; Langner *et al.*, 2001; Ball *et al.*, 2002).

Perpetual Spouter (NGB-PS) and a hot spring from Joseph's Coat Springs (JC3) both exhibit near-neutral pH values, and contain low levels of total soluble Fe (Table 1). However, there are significant differences in the source water chemistry of these two near-neutral pH springs, which result in different geochemical and microbiological processes within the source pools and subsequent outflow channels. The dominant cations and anions in JC3 are  $\text{Na}^+$  (12 mM),  $\text{NH}_4^+$  (5 mM),  $\text{Cl}^-$  (13 mM) and  $\text{SO}_4^{2-}$  (4 mM), and the source waters contain high concentrations of total soluble As (130  $\mu\text{M}$ ), B (5 mM) and Sb (1.5  $\mu\text{M}$ ). Total dissolved sulfide is fairly high ranging from 18 to 32  $\mu\text{M}$  over the last 3 years. Concentrations of other dissolved gases including  $\text{H}_2$  (90–170 nM) and  $\text{CH}_4$  (100–200 nM) are significant and are likely important to chemotrophs inhabiting the source pool and outflow channel. The chemical composition of this spring is stable based on three annual sampling efforts (2002–05), and concentrations of As and Sb are nearly identical to values reported in Stauffer & Thompson (1984).

Perpetual Spouter (NGB-PS) is dominated simply by  $\text{Na}^+$  and  $\text{Cl}^-$ , but contains notable concentrations of B (1.1 mM)

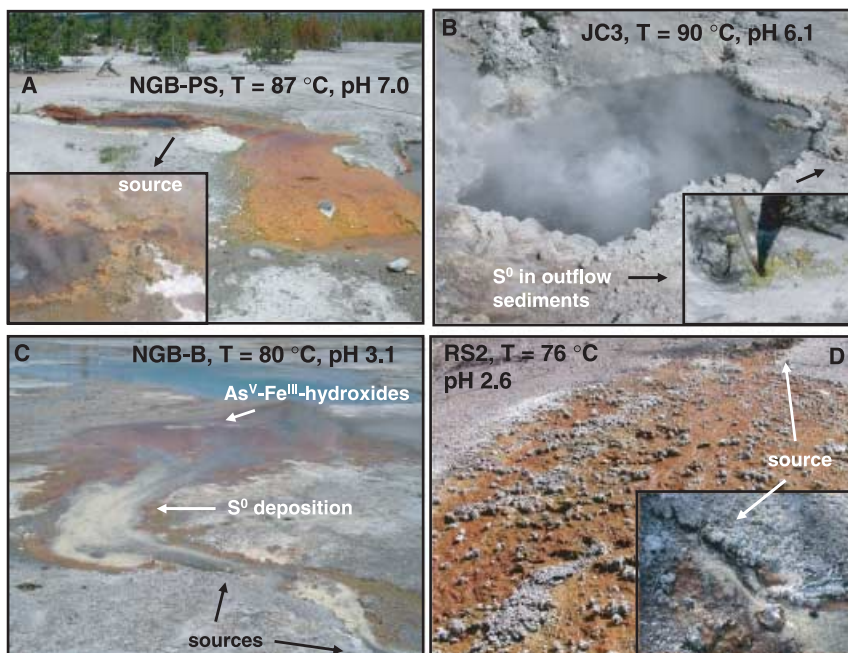


**Fig. 1** Site photographs of subject geothermal springs. (A) Perpetual Spouter, Norris Geyser Basin shows the 3–4 m outflow channel with  $\text{Fe}^{\text{III}}$  oxides deposited along the bottom of the outflow channel and along the rim of the source pool (inset) (photos June 2002). (B) The source pool of Joseph's Coat Springs (JC3) contains pyrite as the primary solid phase, and elemental S in sediments within the outflow channel (inset) (photo July 2004). (C) A representative acid-sulfate-chloride spring from Norris Geyser Basin (NGB-B) shows elemental S deposition (0–3 m from source) followed by accumulation of  $\text{As}^{\text{V}}\text{-Fe}^{\text{III}}$ -oxyhydroxide microbial mats (photo June 2000). (D) Inset shows source discharge of one spring at the Rainbow Springs complex (RS2) with minor accumulation of elemental S from 0 to 30 cm, followed by deposition of  $\text{Fe}^{\text{III}}$ -hydroxides and jarosite in the outflow channel (main picture) (photo July 2004). Temperature and pH values are given for each respective source water.

**Table 1** Average source water chemistry (*total dissolved concentrations*) of case study geothermal Springs from Norris Geyser Basin (NGB), Joseph's Coat (JC) and Rainbow Springs (RS), Yellowstone National Park

Parameter	Unit	Geothermal spring*				
		NGB PS	JC Spring 3	RS Spring 2	NGB Beowulf	NGB Succession
Temperature	°C	87.1	89.8	76.4	75.3	75–84
pH		7.0	6.1	2.6	3.1	3.1
<b>Cations</b>						
Na	mM	21.5	11.5	3.8	12.7	12.5
K	mM	1.5	2.0	2.2	1.2	0.9
Ca	mM	0.27	0.38	0.21	0.13	0.12
Fe	μM	2.7	0.6	97.4	39	60
NH <sub>4</sub>	μM	19.4	5722	1726	65	45
Al	μM	3.8	1.4	290	147	109
Mg	μM	3.4	40.4	82	8.2	9.4
<b>Anions/Neutrals</b>						
Cl	mM	22.7	12.2	0.15	12.7	13.3
SO <sub>4</sub>	mM	0.44	4.3	7.3	1.5	1.3
F	mM	0.36	0.3	0.04	0.16	0.17
Si	mM	5.1	4.0	5.5	4.7	4.82
B	mM	1.1	5.5	0.13	0.65	0.65
†DIC (H <sub>2</sub> CO <sub>3</sub> , HCO <sub>3</sub> <sup>-</sup> )	mM	0.1	0.55	0.74	4.1	2.2
NO <sub>3</sub>	μM	29	9.6	0.3	16	24
As <sup>III</sup>	μM	29	119	3.6	26.6	70–80
As <sup>V</sup>	μM	14	19	0.2	1.4	<1
‡DOC	μM	70	75	45	53	41
§DS(H <sub>2</sub> S, HS <sup>-</sup> )	μM	3.1	20	7.5	131	70
¶CH <sub>4</sub> <sup>g</sup>	μM	bd	0.83	4.2	1.2	1.6
¶H <sub>2</sub> <sup>g</sup>	nM	33	127	31	86	30–60
**CO <sub>2</sub> sat. Index		0.76	1.9	2.3	3.0	2.8
††Ionic strength	mM	24	23	16	17	17

\*Geothermal springs: NGB-PS = Perpetual Spouter, Norris Geyser Basin; JC3 = Joseph's Coat Hot Springs; RS2 = Rainbow Hot Springs; NGB-B = Beowulf Spring, Norris Geyser Basin (Inskeep *et al.*, 2004); NGB-S = Succession Spring, Norris Geyser Basin (Macur *et al.*, 2004a).

†DIC = total dissolved inorganic carbon.

‡DOC = total dissolved organic carbon.

§DS = total dissolved sulfide.

¶Dissolved gas species determined using headspace gas chromatography. bd = below detection, Detection limits = 5 nM for H<sub>2</sub>(aq), 10 nM for CH<sub>4</sub>(aq).

\*\*CO<sub>2</sub> saturation Index = log[CO<sub>2</sub>(aq)/CO<sub>2</sub>(aq, pCO<sub>2</sub> = 0.00035 atm)].

††Ionic strength determined after chemical speciation using MINTeq (Allison *et al.*, 1991) at spring temperature.

and As (40 μM). The concentrations of dissolved sulfide and other dissolved gases including CH<sub>4</sub> and H<sub>2</sub> are considerably lower than the other springs sampled (sulfide ~ 3 μM, H<sub>2</sub>–27 nM and CH<sub>4</sub> is near detection at 10 nM).

All springs contain significant concentrations of dissolved inorganic C (DIC) necessary for supporting autotrophic microbial growth. Values of DIC range from 0.15 to 4 mM in the source waters (Table 1), which correspond to CO<sub>2</sub> supersaturation indices (log[CO<sub>2</sub>(aq)/CO<sub>2</sub>(aq, 0.00035 atm)]) of 0.63 for NGB-PS to nearly 3 for the ASC springs. Consequently, the source waters of these geothermal springs contain from approximately 1–3 orders of magnitude higher CO<sub>2</sub>(aq) than in equilibrium with atmospheric CO<sub>2</sub> (~0.00035 atm).

### Free-energy distribution diagrams

The oxidation–reduction reactions considered in this case study analysis are but a small subset of the possible exergonic reactions that may be important in chemolithotrophic metabolism (Amend & Shock, 2001; Amend *et al.*, 2003). However, the reactions covered here represent a comprehensive range in energy availability from the primary electron donors and acceptors measured in the selected geothermal springs (Table 2), and provide an energetics data set necessary for comparing direct geochemical and microbial observations with the energy availability of exergonic reactions.

Rxn no.	Reaction	* $\Delta G_{\text{rxn}}^{\circ}$ (kJ mol <sup>-1</sup> )
1	H <sub>2</sub> (aq) + 0.5O <sub>2</sub> (aq) = H <sub>2</sub> O	-260.7
2	4H <sub>2</sub> (aq) + NO <sub>3</sub> <sup>-</sup> + 2H <sup>+</sup> = NH <sub>4</sub> <sup>+</sup> + 3H <sub>2</sub> O	-747.5
3	H <sub>2</sub> (aq) + 2Fe <sup>3+</sup> = 2Fe <sup>2+</sup> + 2H <sup>+</sup>	-178.9
4	H <sub>2</sub> (aq) + S <sup>0</sup> = H <sub>2</sub> S(aq)	-47.2
5	4H <sub>2</sub> (aq) + SO <sub>4</sub> <sup>2-</sup> + 2H <sup>+</sup> = H <sub>2</sub> S(aq) + 4H <sub>2</sub> O	-310.3
6	4H <sub>2</sub> (aq) + CO <sub>2</sub> (aq) = CH <sub>4</sub> (aq) + 2H <sub>2</sub> O	-186.9
7	H <sub>2</sub> (aq) + H <sub>3</sub> AsO <sub>4</sub> = H <sub>3</sub> AsO <sub>3</sub> + H <sub>2</sub> O	-128.8
8	H <sub>2</sub> S(aq) + 0.5O <sub>2</sub> (aq) = S <sup>0</sup> + H <sub>2</sub> O	-213.4
9	H <sub>2</sub> S(aq) + 2O <sub>2</sub> (aq) = SO <sub>4</sub> <sup>2-</sup> + 2H <sup>+</sup>	-732.3
10	H <sub>2</sub> S(aq) + H <sub>3</sub> AsO <sub>4</sub> = S <sup>0</sup> + H <sub>3</sub> AsO <sub>3</sub> + H <sub>2</sub> O	-81.6
11	H <sub>2</sub> S(aq) + H <sub>2</sub> AsO <sub>4</sub> <sup>-</sup> + H <sup>+</sup> = S <sup>0</sup> + H <sub>3</sub> AsO <sub>3</sub> + H <sub>2</sub> O	-97.9
12	H <sub>2</sub> S(aq) + 2Fe <sup>3+</sup> = S <sup>0</sup> + 2Fe <sup>2+</sup> + 2H <sup>+</sup>	-131.6
13	H <sub>2</sub> S(aq) + 0.25NO <sub>3</sub> <sup>-</sup> + 0.5H <sup>+</sup> = S <sup>0</sup> + 0.25NH <sub>4</sub> <sup>+</sup> + 0.75H <sub>2</sub> O	-139.7
14	S <sup>0</sup> + 1.5O <sub>2</sub> (aq) + H <sub>2</sub> O = SO <sub>4</sub> <sup>2-</sup> + 2H <sup>+</sup>	-518.9
15	S <sup>0</sup> + 3H <sub>3</sub> AsO <sub>4</sub> + H <sub>2</sub> O = SO <sub>4</sub> <sup>2-</sup> + 3H <sub>3</sub> AsO <sub>3</sub> + 2H <sup>+</sup>	-123.4
16	S <sup>0</sup> + 3H <sub>2</sub> AsO <sub>4</sub> <sup>-</sup> + H <sub>2</sub> O + H <sup>+</sup> = SO <sub>4</sub> <sup>2-</sup> + 3H <sub>3</sub> AsO <sub>3</sub>	-172.2
17	S <sup>0</sup> + 6Fe <sup>3+</sup> + 4H <sub>2</sub> O = SO <sub>4</sub> <sup>2-</sup> + 6Fe <sup>2+</sup> + 8H <sup>+</sup>	-273.5
18	S <sup>0</sup> + 6Fe(OH) <sub>3</sub> + 10H <sup>+</sup> = SO <sub>4</sub> <sup>2-</sup> + 6Fe <sup>2+</sup> + 14H <sub>2</sub> O	-335.5
19	S <sup>0</sup> + 0.75NO <sub>3</sub> <sup>-</sup> + H <sub>2</sub> O + 2H <sup>+</sup> = SO <sub>4</sub> <sup>2-</sup> + 0.75NH <sub>4</sub> <sup>+</sup>	-478.0
20	H <sub>3</sub> AsO <sub>3</sub> + 0.5O <sub>2</sub> (aq) = H <sub>2</sub> AsO <sub>4</sub> <sup>-</sup> + H <sup>+</sup>	-115.6
21	4H <sub>3</sub> AsO <sub>3</sub> + NO <sub>3</sub> <sup>-</sup> + H <sub>2</sub> O = 4H <sub>2</sub> AsO <sub>4</sub> <sup>-</sup> + NH <sub>4</sub> <sup>+</sup> + 2H <sup>+</sup>	-167.2
22	H <sub>3</sub> AsO <sub>3</sub> + 2Fe <sup>3+</sup> + H <sub>2</sub> O = 2Fe <sup>2+</sup> + H <sub>3</sub> AsO <sub>4</sub> + 2H <sup>+</sup>	-50.0
23	H <sub>3</sub> AsO <sub>3</sub> + 2Fe(OH) <sub>3</sub> + 3H <sup>+</sup> = 2Fe <sup>2+</sup> + H <sub>2</sub> AsO <sub>4</sub> <sup>-</sup> + 5H <sub>2</sub> O	-52.5
24	2Fe <sup>2+</sup> + 0.5O <sub>2</sub> (aq) + 2H <sup>+</sup> = 2Fe <sup>3+</sup> + H <sub>2</sub> O	-81.8
25	Fe <sup>2+</sup> + 0.25O <sub>2</sub> (aq) + 2.5H <sub>2</sub> O = Fe(OH) <sub>3</sub> (s) + 2H <sup>+</sup>	-30.9
26	8Fe <sup>2+</sup> + NO <sub>3</sub> <sup>-</sup> + 10H <sup>+</sup> = NH <sub>4</sub> <sup>+</sup> + 8Fe <sup>3+</sup> + 3H <sub>2</sub> O	-32.1
27	8Fe <sup>2+</sup> + NO <sub>3</sub> <sup>-</sup> + 21H <sub>2</sub> O = NH <sub>4</sub> <sup>+</sup> + 8Fe(OH) <sub>3</sub> (s) + 14H <sup>+</sup>	+49
28	CH <sub>4</sub> (aq) + 2O <sub>2</sub> (aq) = CO <sub>2</sub> (aq) + 2H <sub>2</sub> O	-855.8
29	CH <sub>4</sub> (aq) + SO <sub>4</sub> <sup>2-</sup> + 2H <sup>+</sup> = CO <sub>2</sub> (aq) + H <sub>2</sub> S(aq) + 2H <sub>2</sub> O	-123.5
30	CH <sub>4</sub> (aq) + NO <sub>3</sub> <sup>-</sup> + 2H <sup>+</sup> = CO <sub>2</sub> (aq) + NH <sub>4</sub> <sup>+</sup> + H <sub>2</sub> O	-560.7
31	CH <sub>4</sub> (aq) + 8Fe <sup>3+</sup> + 2H <sub>2</sub> O = CO <sub>2</sub> (aq) + 8Fe <sup>2+</sup> + 8H <sup>+</sup>	-528.6
32	CH <sub>4</sub> (aq) + 4H <sub>2</sub> AsO <sub>4</sub> <sup>-</sup> + 4H <sup>+</sup> = CO <sub>2</sub> (aq) + 4H <sub>3</sub> AsO <sub>3</sub> + 2H <sub>2</sub> O	-400.6
33	NH <sub>4</sub> <sup>+</sup> + 2O <sub>2</sub> (aq) = NO <sub>3</sub> <sup>-</sup> + 2H <sup>+</sup> + H <sub>2</sub> O	-295.1

\*Standard state free-energy values [ $\Delta G_{\text{rxn}}^{\circ}$ (kJ mol<sup>-1</sup>)] are given at a temperature of 70 °C.

Free-energy values (kJ per mol electron) for the exergonic reactions given in Table 2 are examined in energy distribution diagrams for each spring (Fig. 2). The distribution of  $\Delta G_{\text{rxn}}$  values over these selected redox couples exhibits the common shape of a theoretical electron titration. For example, the oxidation of H<sub>2</sub> is most exergonic when O<sub>2</sub> is the electron donor, followed in general order by NO<sub>3</sub><sup>-</sup>, Fe<sup>III</sup>, As<sup>V</sup>, S<sup>0</sup>, SO<sub>4</sub><sup>2-</sup> and CO<sub>2</sub> (Fig. 2B). With O<sub>2</sub> as a constant electron acceptor, the calculated free-energy values are highest when H<sub>2</sub> serves as the electron donor followed by reactions with C<sup>-IV</sup>, S<sup>-II</sup>, As<sup>III</sup>, Fe<sup>II</sup> and N<sup>-III</sup> (Fig. 2C). These trends are generally as expected across a relevant range of earth-surface temperatures (0–100 °C) (Stumm & Morgan, 1996; Amend & Shock, 2001; Madigan *et al.*, 2003), because the redox couples are poised at discrete free energies defined in large part by the standard state free-energy value and the pH. The specific spring conditions have an important modifying effect on calculated free-energy values, but as will be shown in sensitivity analyses (Figs 6,7), the range in calculated  $\Delta G_{\text{rxn}}$  values is often tightly constrained by the standard state value

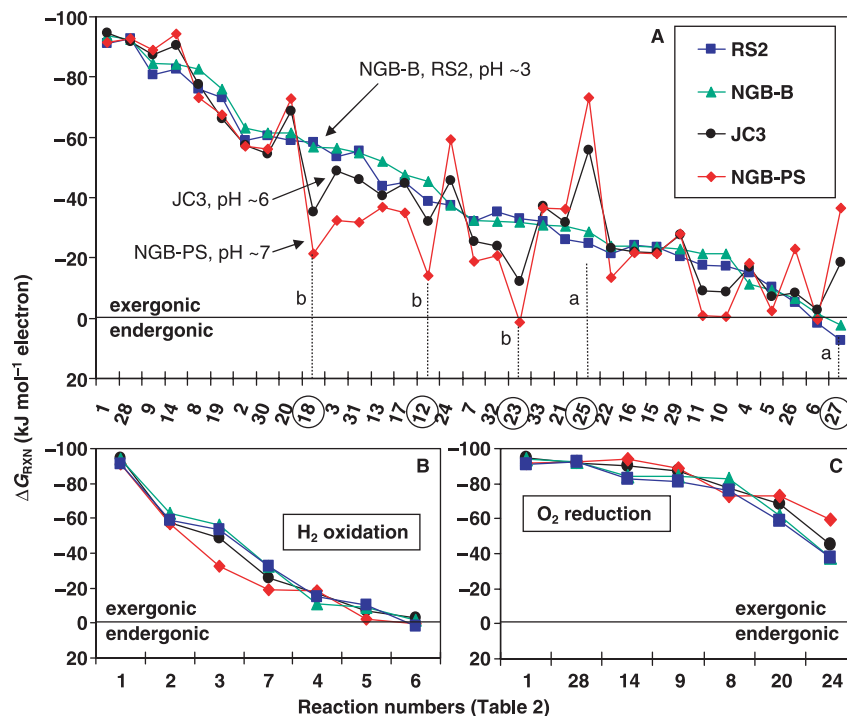
and a plausible range in the activities of oxidized and reduced species.

Free-energy values for the acidic springs (RS2 and NGB-B) track closely across the 33 redox reactions considered (Fig. 2A). Variation in reaction free-energy values between acidic and near-neutral springs was significant for reactions with pH dependence. For example, reactions involving H<sup>+</sup> as a product were often considerably more favourable at higher pH in JC3 and NGB-PS (e.g. reactions 25 and 27 marked with a in Fig. 2A). Conversely, H<sup>+</sup>-consuming reactions, such as reactions 12, 18 and 23, were generally more favourable in acidic springs (marked with b in Fig. 2A). Reaction 12 (b in Fig. 2A) involving the oxidation of H<sub>2</sub>S with Fe<sup>3+</sup> is less exergonic at high pH due primarily to the fact that calculated Fe<sup>3+</sup> activities drop considerably (6–8 orders of magnitude) at pH values of 6–7.

It is clear from the energy distribution profile of these springs that despite differences in chemistry and subsequent geochemical processes, variations in reaction free energies for many reactions do not exceed 5–10 kJ mol<sup>-1</sup> electron.

**Table 2** Oxidation–reduction reactions considered in energetic analyses of potential chemolithotrophic metabolisms within YNP geothermal springs. Reactions are written with the electron donor as the first reactant and the electron acceptor as the second reactant

**Fig. 2** (A) Free-energy values ( $\Delta G_{\text{rxn}}$ ,  $\text{kJ mol}^{-1}$  electron) for 33 electron transfer reactions given in Table 2, calculated at source pool conditions for four geothermal springs in YNP. Reactions with  $\text{O}_2(\text{aq})$  as an electron acceptor (e.g. Reactions 1, 8, 9, 14, 20, 28) generally yield the highest free-energy values for all sites. Major differences in  $\Delta G_{\text{rxn}}$  for specific reactions among different geothermal springs can be traced directly to changes in  $\text{H}^+$  activity and/or the strong pH dependence of  $\text{Fe}^{3+}$  activity (e.g. see Reactions 12, 18, 23, 25, 27 [labelled a and b in diagram]). (B) Redox reactions for  $\text{H}_2$  oxidation show expected declines in reaction free energies as a function of different electron acceptors ( $\text{O}_2$ ,  $\text{NO}_3^-$ ,  $\text{Fe}^{\text{III}}$ ,  $\text{As}^{\text{V}}$ ,  $\text{S}^{\circ}$ ,  $\text{SO}_4^{2-}$ , and  $\text{CO}_2$ ). (C) Redox reactions where  $\text{O}_2$  serves as the electron acceptor show expected declines in free energy as a function of different electron donors ( $\text{H}_2$ ,  $\text{CH}_4$ ,  $\text{H}_2\text{S}$ ,  $\text{As}^{\text{III}}$ ,  $\text{Fe}^{\text{II}}$  and  $\text{NH}_4^+$ ).



Reactions involving  $\text{H}^+$  or species highly dependent on  $\text{H}^+$  (e.g.  $\text{Fe}^{3+}$  activity) exhibit greater differences of up to  $40 \text{ kJ mol}^{-1}$  electron between acidic and near-neutral sites. For example, reactions with Fe often exhibit the greatest variation in free-energy values among sites, and local geochemical conditions can more likely have an impact on whether a specific Fe reaction is exergonic vs. endergonic (Fig. 2A). The absolute magnitude and ranges in free-energy values observed in the YNP geothermal systems (Fig. 2) are similar to those reported by Amend *et al.* (2003) for the hydrothermal systems of Vulcano Island. In part, this is due to the fact that the reactions are poised by their standard state free-energy values, and due to the similar pH range of the 10 Vulcano Island sites (pH range  $\sim 2$ – $6.3$ ). Both studies show that the energetic calculations do not change the outcome that a similar set of redox reactions are highly exergonic in all sites and may provide energy for chemotrophic metabolism. Examination of the actual geochemical processes and microbial populations occurring in the springs can further elucidate which exergonic reactions may be most relevant.

### Observed geochemical gradients and microbial populations

#### Nonequilibrium systems

The YNP geothermal source waters discussed here are nonequilibrium systems in two important respects. First, the source waters generally exhibit significant oversaturation of dissolved gas species such as  $\text{CO}_2$ ,  $\text{H}_2$ ,  $\text{CH}_4$  and  $\text{H}_2\text{S}$ , whereas dissolved oxygen values are generally undersaturated with

respect to earth surface conditions (e.g.  $\text{pO}_2 \sim 0.2 \text{ atm}$ ). Second, the geothermal source waters exhibit significant redox nonequilibrium and contain various amounts of reduced constituents dependent in part on the degree of meteoric water mixing and oxygenation prior to discharge (Fournier, 1989).

The redox nonequilibrium of geothermal source waters can be illustrated by comparing values of  $\text{pe}$  ( $-\log$  electron activity) calculated using individual half-cell reactions as a function of distance throughout the outflow channels (Fig. 3). Although temperature effects are accounted for in these calculations, the temperature changes occurring within these sampling zones (e.g.  $80$ – $55 \text{ }^\circ\text{C}$ ) do not have a significant impact on the calculated  $\text{pe}$  values, or the free-energy values to be discussed further. This point has been noted in Amend & Shock (2001) and in Amend *et al.* (2003). The calculated  $\text{pe}$  values for a given half-cell reaction are poised by their respective standard state  $\text{pe}^\circ$  values, and by a plausible window of observation ranging from analytical detection to realistic upper concentration limits. For example, the  $\text{pe}^\circ$  value for the hydrogen half-cell ( $\text{H}^+ + \text{e}^- = 1/2\text{H}_2(\text{aq})$ ) ranges from  $-1$  to  $-1.25$  from  $85$  to  $55 \text{ }^\circ\text{C}$ ; the calculated  $\text{pe}$  values are poised at  $\sim 0$  for the acidic systems (pH $\sim 3$ ) and at  $\sim -3$  for the near-neutral systems (Fig. 3). Conversely, the oxygen half-cell ( $0.25\text{O}_2(\text{aq}) + \text{H}^+ + \text{e}^- = 0.5 \text{H}_2\text{O}$ ) is poised near  $\text{pe}$  values of  $10$ – $15$  (Fig. 3) over the same pH range. The chemical component that is most singly responsible for differences in calculated  $\text{pe}$  values among springs is  $\text{H}^+$  activity, which explains the 3–4 order-of-magnitude shift in electron activity observed comparing low pH (NGB-B,

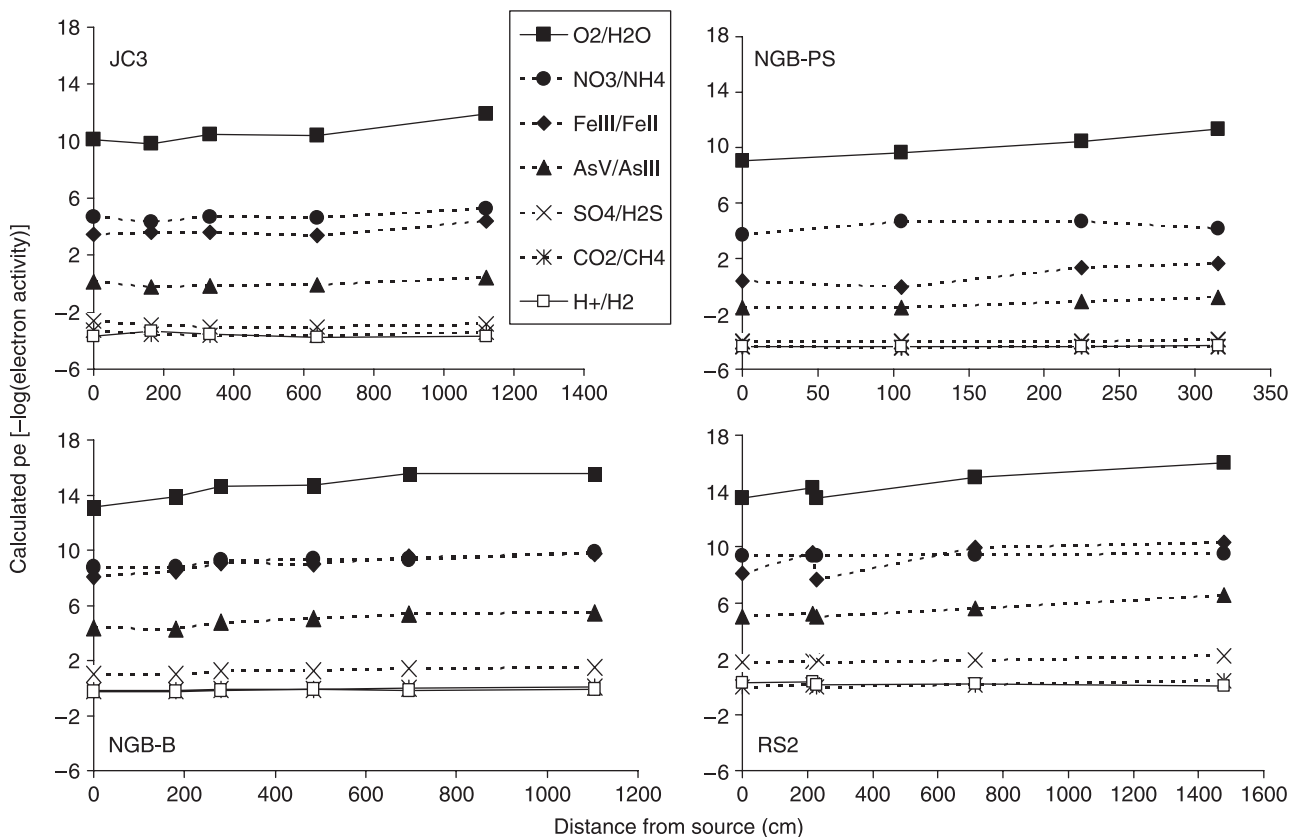


**Fig. 3** Calculated  $pe$  ( $-\log[\text{electron activity}]$ ) values for seven half-cell reactions involving redox active species present in geothermal source waters ( $\text{O}_2/\text{H}_2\text{O}$ ,  $\text{NO}_3^-/\text{NH}_4^+$ ,  $\text{Fe}^{3+}/\text{Fe}^{2+}$ ,  $\text{H}_2\text{AsO}_4^-/\text{H}_3\text{AsO}_3$ ,  $\text{SO}_4^{2-}/\text{H}_2\text{S}$ ,  $\text{CO}_2/\text{CH}_4$ ,  $\text{H}^+/\text{H}_2$ ) plotted as a function of distance within the outflow channel of four geothermal springs in YNP. Significant redox nonequilibrium is observed in all springs. A shift in  $pe$  values at 210–230 cm in RS2 corresponds to a second geothermal source contributing reduced chemical inputs to the main channel, essentially creating a duplicate of source water conditions at 0 cm.

NGB-S, RS2) vs. neutral pH (JC3, NGB-PS) systems (Fig. 3). Geochemical transformations occurring in the outflow channels of these springs (discussed below) are not readily apparent when examining changes in individually calculated  $pe$  values as a function of distance.

The  $pe$  calculations also clarify that there is no ‘system’  $pe$  that would adequately describe the ratios of all oxidized to reduced species. For example, the range of  $pe$  values observed (Fig. 3) for the predominant redox pairs ( $\text{O}_2/\text{H}_2\text{O}$ ,  $\text{H}^+/\text{H}_2$ ,  $\text{SO}_4^{2-}/\text{H}_2\text{S}$ ,  $\text{H}_2\text{AsO}_4^-/\text{H}_3\text{AsO}_3$ ,  $\text{Fe}^{3+}/\text{Fe}^{2+}$ ,  $\text{CO}_2/\text{CH}_4$ ,  $\text{NO}_3^-/\text{NH}_4^+$ ) spans nearly 14 orders of magnitude throughout the outflow channel of each geothermal spring considered! Given the lack of redox equilibrium among half-cell reactions, platinum  $E_{\text{H}}$  values are of limited use in describing or representing the redox status of geothermal waters, or for that matter, any natural system. These points have been emphasized in previous literature (Stumm, 1984; Stumm & Morgan, 1996), but it should be reiterated that measurements of oxidized and reduced species are far more insightful than measurements of  $E_{\text{H}}$  for evaluating chemolithotrophic processes, and for determining the potential importance of specific redox couples in geothermal systems.

#### *Geochemical gradients resulting from air–water gas exchange*

The rates of degassing of  $\text{H}_2\text{S}$ ,  $\text{CO}_2$ ,  $\text{CH}_4$  and  $\text{H}_2$ , combined with the rate of  $\text{O}_2$  ingassing are among the most important processes defining geochemical gradients and diverse microbial habitats as a function of distance within the outflow channels (Fig. 4). The rates of degassing or ingassing at specific distances within the outflow channels are dependent on physical factors including stream velocity, air–water surface area and boundary layer turbulence (Choi *et al.*, 1998; Jähne & Haussbecker, 1998). For some components ( $\text{H}_2\text{S}$  and  $\text{CO}_2$ ), pH plays a major role in defining the distribution of aqueous species, which can have a major effect on subsequent degassing rates. For example, in low pH systems such as RS2, NGB-B and NGB-S,  $\text{H}_2\text{S}(\text{aq})$  is the dominant chemical species comprising total dissolved sulfide. Consequently, the rates of degassing are rapid and within 4–6 m of discharge, dissolved sulfide values decline to less than 5% of source water values (also see Nordstrom *et al.*, 2005). Conversely, at a pH of 6.1 (close to the  $\text{pK}_a$  of  $\text{H}_2\text{S}(\text{aq})$ ), dissolved sulfide values in JC3 only decline to 50% of source water values by 10 m. This is due in large part to the fact that  $\text{HS}^-$  becomes an

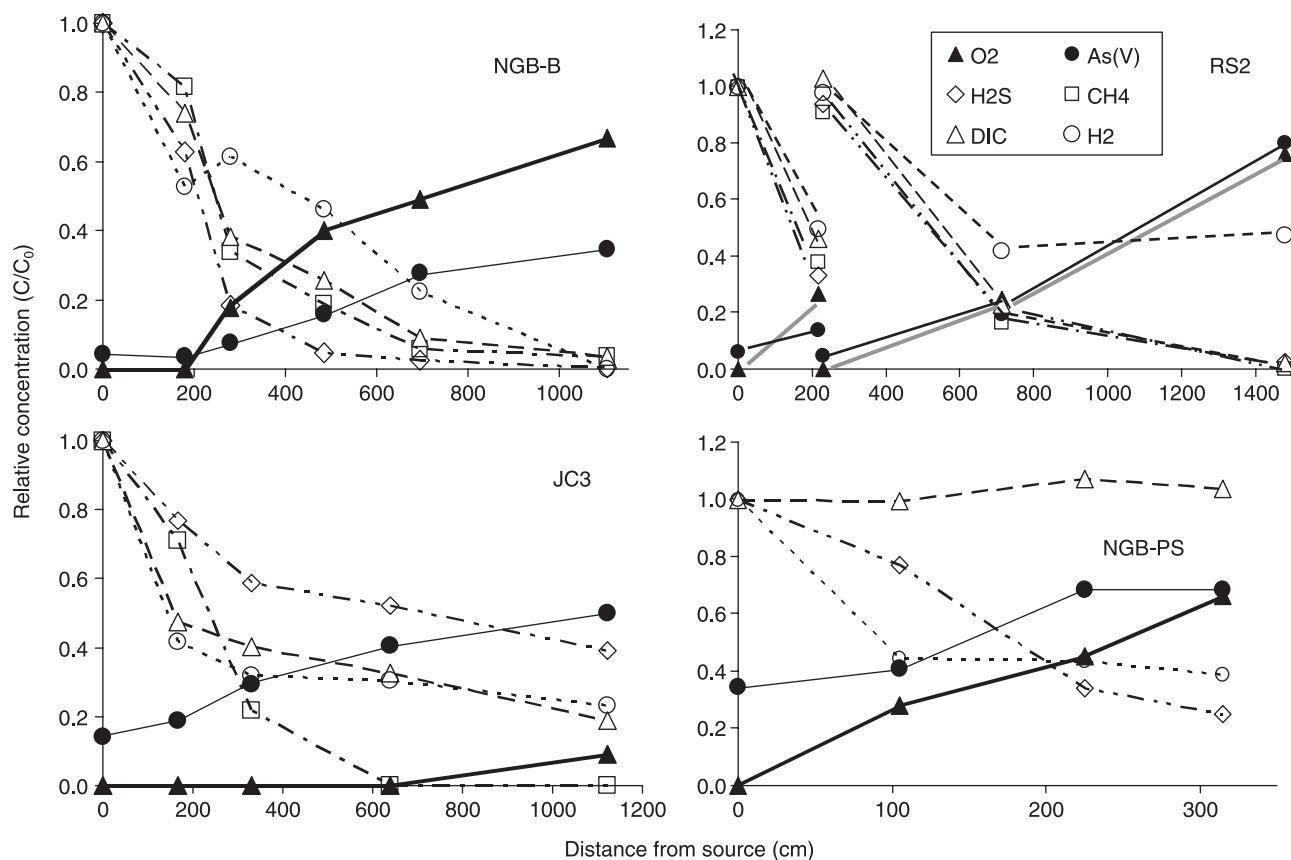


**Fig. 4** Concentrations of dissolved gases and As<sup>V</sup> as a function of distance within the outflow channel plotted as a fraction of the total concentration observed within the source pool ( $C/C_0$ ). Values of  $C_0$  for dissolved inorganic C (DIC), H<sub>2</sub>(aq), total dissolved sulfide, CH<sub>4</sub>(aq), and total soluble As are given in Table 1. The  $C_0$  used for dissolved O<sub>2</sub> is the calculated O<sub>2</sub>(aq) in equilibrium with the atmosphere at this temperature and total pressure. The discontinuity shown for RS2 corresponds to a second geothermal source water input at 210 cm.

important soluble species at pH ~ 6. Likewise, the disappearance rates of dissolved inorganic C (DIC) are highly dependent on pH. In the acidic springs (NGB-B, NGB-S and RS2), >99% of the DIC is present as CO<sub>2</sub>(aq) and disappearance rates are rapid (Fig. 4). Conversely, the loss in DIC as a function of distance is less rapid for JC3 (pH ~ 6) and not significant at all across a 3-m interval in Perpetual Spouter (NGB-PS) at a pH near 7 (Fig. 4). In the low pH springs (pH ~ 3), the disappearance rates are similar for all dissolved gases including H<sub>2</sub>S, CO<sub>2</sub>, CH<sub>4</sub> and H<sub>2</sub>, suggesting that mass transfer across the air–water interface is likely the dominant process controlling the distribution of these chemical species down gradient.

#### Arsenic oxidation

Arsenite (As<sup>III</sup>) is oxidized to arsenate (As<sup>V</sup>) within the outflow channels of all springs studied (Fig. 4). The oxidation of As<sup>III</sup> in ASC springs (NGB-B, NGB-S, NGB-D) is extremely rapid (first-order rate constants ranging from 1 to 5 min<sup>-1</sup>) and has been shown to be microbially mediated where 40–100% of the soluble As<sup>III</sup> is oxidized to As<sup>V</sup> across a temperature range of ~75–55 °C (Langner *et al.*, 2001;

Inskeep *et al.*, 2004; Macur *et al.*, 2004a). At least one isolate (a *Hydrogenobaculum acidophilum*-like organism) capable of oxidizing As<sup>III</sup> has been obtained from the ASC springs of Norris Geyser Basin and dissolved sulfide inhibits enzymatic oxidation of As<sup>III</sup> by this organism (Donahoe-Christiansen *et al.*, 2004). This agrees with *in situ* observations that As<sup>III</sup> oxidation is not significant in the ASC springs until H<sub>2</sub>S(aq) levels drop below ~5 μM. The extent and rate of As<sup>III</sup> oxidation in RS2 and NGB-PS are also significant and generally correlate with O<sub>2</sub> ingassing (Fig. 4). Finally, As<sup>III</sup> oxidation is important even in JC3 where total dissolved sulfide drops from approximately 30 μM in the source waters to ~10–12 μM within 10–11 m down gradient (Fig. 4).

#### Solid phase deposition

Solid phases are deposited in the source pools and throughout the outflow channels of all springs studied (Table 3). In the acid–sulfate (RS2) and acid–sulfate–chloride (NGB-B, NGB-S, NGB-D) springs, deposition of S<sup>0</sup> occurs at the source and within the outflow channel until H<sub>2</sub>S levels drop below ~3–5 μM. Given the higher levels of total dissolved sulfide in the ASC springs, S<sup>0</sup> is more abundant in the outflow channels

**Table 3** Predominant solid phases formed within source pools and/or outflow channels of several geothermal springs in YNP

Thermal spring	Distance from source (m)	Temperature range (°C)	Predominant solid phases*
NGB-B, S	0–3, 0–4 m	60–85	Elemental S <sup>0</sup>
	3–6, 4–10 m	50–65	As <sup>V</sup> – Fe <sup>III</sup> oxides
RS2	0–0.5 m	70–75	Elemental S <sup>0</sup> and high K-Al silicate
	Outflow channel	50–70	Fe <sup>III</sup> oxides, jarosite
JC3	0 m (source pool)	75–90	FeS <sub>2</sub> , S <sup>0</sup> , SbS <sub>x</sub>
	Outflow Channel	50–75	SiO <sub>x</sub> , alunite, S <sup>0</sup> , As <sub>2</sub> S <sub>3</sub>
NGB-PS	0 m (source pool)	80–85	SiO <sub>x</sub> , Fe <sup>III</sup> oxides
	Outflow Channel	60–75	SiO <sub>x</sub> , Fe <sup>III</sup> oxides

\*Determined using X-ray diffraction (XRD), total solid phase dissolution, and scanning electron microscopy coupled with energy dispersive analysis of X-rays (SEM-EDAX) (Inskeep *et al.*, 2004; Macur *et al.*, 2004a; W.P. Inskeep, unpublished data).

(0–3 m, Fig. 1C,D), creating an environment where organisms capable of metabolism involving S<sup>0</sup> could potentially flourish. Conversely, RS2 exhibits only traces of elemental S lining the channel floor for short distances from each source (0–30 cm, and 230–250 cm). Elemental S also accumulates within the softer sediments of JC3, where dissolved sulfide levels remain above 10 μM throughout the region of outflow channel studied (Fig. 1B). No elemental S has been observed within the neutral spring (NGB-PS) containing only 3 μM dissolved sulfide at the source.

Iron solid phases figure prominently in all springs studied. In the ASC springs, hydrous ferric oxide (HFO) phases form an abrupt boundary down gradient of elemental S deposition (Fig. 1) at approximately 5–12 m in NGB-B and NGB-S (Inskeep *et al.*, 2004; Macur *et al.*, 2004a). The Fe microbial mats are comprised primarily of filaments encrusted with poorly ordered ferrihydrite-like phases containing arsenate (0.7 mol As:mol Fe) complexed to Fe<sup>III</sup>-octahedral sites (Inskeep *et al.*, 2004). Amorphous Fe<sup>III</sup> oxides also form in RS2, just down gradient of each of the shorter H<sub>2</sub>S zones corresponding to source water contributions at 0 cm and at 230 cm (Fig. 4); however, these Fe phases do not exhibit an As signature due to the relatively low concentration of source water As (~3 μM). Jarosite (KFe<sub>3</sub>(SO<sub>4</sub>)<sub>2</sub>(OH)<sub>6</sub>) is an important solid phase in the Fe mats of RS2 where higher concentrations of sulfate and aqueous Fe<sup>III</sup> (likely due to the microbial oxidation of Fe<sup>II</sup>) yield conditions suitable for the formation of well-ordered K-jarosite (Table 3).

Despite low concentrations of soluble Fe in the near-neutral geothermal springs (JC3 and NSG-PS), Fe solid phases are important in both systems. In NGB-PS, Fe<sup>III</sup>-oxides form as hard coatings on SiO<sub>2</sub> phases surrounding the source pool, and as soft microbial mats in the outflow channel from temperatures of 85–65 °C (Fig. 1A). Although there is a significant amount of soluble As<sup>V</sup> present in NGB-PS, the Fe-oxide phases do not contain significant quantities of As. This is likely due to the pH dependence and resultant competitive complexation of silicate and arsenate binding for surface Fe-O sites (Meng *et al.*, 2000; Davis *et al.*, 2001). Conversely, pyrite

(FeS<sub>2</sub>) is the dominant Fe phase formed in the source pool of JC3 (Fig. 1B), and no evidence of significant Fe oxidation is exhibited throughout the outflow channel. This may be due in part to the slower rate of H<sub>2</sub>S degassing and O<sub>2</sub> ingassing in JC3 (Fig. 4). Energetic analyses of the source waters of these two springs indicated that both the oxidation of Fe<sup>II</sup> and the reduction of Fe<sup>III</sup> was exergonic, but that reduction of Fe<sup>III</sup> via H<sub>2</sub> was favoured in JC3 relative to NGB-PS.

In summary, gas exchange rates and spring water velocity define zones of H<sub>2</sub>, CH<sub>4</sub>, H<sub>2</sub>S and CO<sub>2</sub> degassing as well as O<sub>2</sub> ingassing. Although air–water gas exchange rates are controlled by abiotic processes, they have a substantial impact on the solid phase geochemistry and the types of microbial communities that develop throughout the outflow channels. The solid phases formed in these microbial mats may often reveal clues regarding important microbial metabolisms operative *in situ*. The deposition of elemental S, for example, appears to only occur when total dissolved sulfide concentrations exceed ~5 μM (at least at these spring velocities), and this zone is in large part defined by the degassing of H<sub>2</sub>S(aq). It is also clear that Fe-oxide mats develop upon significant oxygenation due to ingassing and are not likely to form in the presence of dissolved sulfide >2–3 μM. Conversely in JC3, the presence of dissolved sulfide and the resultant slower ingassing of O<sub>2</sub> (Fig. 4) encourages the formation of pyrite (FeS<sub>2</sub>).

#### Microbial population distribution

The distribution of observed 16S rRNA gene sequences in these geothermal springs is summarized in Table 4, where the predominant sequences with close cultivated relatives are presented as a function of distance within the outflow channel. Although not all sampling sites are listed for each spring, this description summarizes several of the major changes in phylogeny that occur in the solid phases and microbial mats found near the source waters or down gradient in the outflow channels. The possible metabolisms of organisms represented by these sequences are listed to suggest potential roles for these organisms in mediating geochemical processes observed *in situ*. It is important to note that in all springs, additional

**Table 4** Summary of 16S rDNA sequence types\* identified in the prominent zones of YNP geothermal springs indicated by the closest cultivated relatives, phylogenetic affiliation, GenBank Accession numbers and possible metabolisms at specific spring locations based on geochemical conditions and known physiologies of cultivated relatives

Spring	Spring location <sup>†</sup>	Genus of nearest cultivated relative <sup>‡</sup>	Phylogenetic group	Accession number	Possible metabolism <sup>¶</sup>	
					Donors	Acceptors
Acidic Spring	H <sub>2</sub> S, S <sup>0</sup> zone 75–84 °C	<i>Stygiolobus</i> (98)	Crenarchaeota	AY191883	H <sub>2</sub>	S <sup>0</sup>
		<i>Caldococcus</i> (97)	Crenarchaeota	AY191881	OC**	S <sup>0</sup>
		<i>Thermocladium</i> (98)	Crenarchaeota	AY191886	OC	S <sup>0</sup>
NGB-D		<i>Caldisphaera</i> (96)	Crenarchaeota	AY191890	OC	S <sup>0</sup>
NGB-S	H <sub>2</sub> S, S <sup>0</sup> zone 60–75 °C	<i>Hydrogenobaculum</i> (99)	Aquificales	AY191873	H <sub>2</sub> , S <sup>0</sup> , As <sup>III</sup>	O <sub>2</sub>
		<i>Desulfurella</i> (97)	δ-Proteobacteria	AF325180	OC	S <sup>0</sup> , SO <sub>4</sub>
	As <sup>V</sup> -Fe(OH) <sub>3</sub> 50–65 °C	<i>Hydrogenobaculum</i> (99)	Aquificales	AY191874	H <sub>2</sub> , As <sup>III</sup> ?**	O <sub>2</sub>
		<i>Metallosphaera</i> (98)	Crenarchaeota	AY191884	Fe <sup>II</sup> , S <sup>0</sup>	O <sub>2</sub>
		<i>Sulfobacillus</i> (98)	Firmicutes	DQ350778	Fe <sup>II</sup> , S <sup>0</sup>	O <sub>2</sub>
		<i>Thiomonas</i> (98)	β-Proteobacteria	AY191879	Fe <sup>II</sup> , S <sup>0</sup> , As <sup>III</sup>	O <sub>2</sub>
		<i>Acidimicrobium</i> (98)	Actinobacteria	AY191899	OC, Fe <sup>II</sup>	O <sub>2</sub> , Fe <sup>III</sup>
Acetobacteraceae Y008 (99)	α-Proteobacteria	AY191880	OC	O <sub>2</sub> , Fe <sup>III</sup>		
Acidic Spring	H <sub>2</sub> S, S <sup>0</sup> zone 70–75 °C	<i>Stygiolobus</i> (99)	Crenarchaeota	AY191882	H <sub>2</sub>	S <sup>0</sup>
		<i>Hydrogenobaculum</i> (99)	Aquificales	AY882797	H <sub>2</sub> , S <sup>0</sup> , As <sup>III</sup>	O <sub>2</sub>
		<i>Metallosphaera</i> (96)	Crenarchaeota	AY882800	S <sup>0</sup> , Fe <sup>II</sup>	O <sub>2</sub>
RS2	Fe(OH) <sub>3</sub> , jarosite 55–70 °C	<i>Hydrogenobaculum</i> (98)	Aquificales	AY882804	H <sub>2</sub> , S <sup>0</sup> , As <sup>III</sup>	O <sub>2</sub>
		<i>Metallosphaera</i> (96)	Crenarchaeota	AY882806	Fe <sup>II</sup> , S <sup>0</sup>	O <sub>2</sub>
		<i>Acidianus</i> (93)	Crenarchaeota	AY882801	Fe <sup>II</sup> , S <sup>0</sup>	O <sub>2</sub>
		<i>Metallosphaera</i> (95)	Crenarchaeota	AY882814	Fe <sup>II</sup> , S <sup>0</sup>	O <sub>2</sub>
		<i>Sulfobacillus</i> (93)	Firmicutes	AY882815	Fe <sup>II</sup>	O <sub>2</sub>
		Acetobacteraceae Y008 (98)	α-Proteobacteria	AY882809	OC	O <sub>2</sub> , Fe <sup>III</sup>
Neutral Spring	FeS <sub>2</sub> , <sup>§</sup> SbS <sub>x</sub> 75–90 °C	<i>Geothermobacterium</i> (99)	Thermodesulfobacteria	AY882717	H <sub>2</sub>	Fe <sup>III</sup>
		<i>Vulcanisaeta</i> (97)	Crenarchaeota	AY882719	OC	S <sub>2</sub> O <sub>3</sub> , S <sup>0</sup>
		<i>Caldococcus</i> (97)	Crenarchaeota	AY882714	OC	S <sup>0</sup>
		<i>Thermofilum</i> (94)	Crenarchaeota	AY882718	OC	S <sup>0</sup>
JC3	SiO <sub>2</sub> , S <sup>0</sup> 50–75 °C	<i>Caldococcus</i> (96)	Crenarchaeota	AY882764	OC	S <sup>0</sup>
		<i>Caldisphaera</i> (97)	Crenarchaeota	DQ333311	OC	S <sup>0</sup>
		<i>Desulfurella</i> (98)	δ-Proteobacteria	DQ333312	OC	S <sup>0</sup> , SO <sub>4</sub>
		<i>Sulfurihydrogenibium</i> (98)	Aquificales	AY882757	H <sub>2</sub> , S <sub>2</sub> O <sub>3</sub> , S <sup>0</sup>	O <sub>2</sub> , NO <sub>3</sub> <sup>-</sup>
		<i>Thermocrinis</i> (98)	Aquificales	AY882760	H <sub>2</sub> , S <sub>2</sub> O <sub>3</sub> , S <sup>0</sup>	O <sub>2</sub>
		<i>Thermus</i> (99)	<i>Deinococcus-Thermus</i>	AY882763	OC, As <sup>III</sup> ?	O <sub>2</sub>
Neutral Spring	SiO <sub>2</sub> , Fe(OH) <sub>3</sub> 80–85 °C	<i>Thermocrinis</i> (99)	Aquificales	DQ324878	H <sub>2</sub> , S <sub>2</sub> O <sub>3</sub> , S <sup>0</sup>	O <sub>2</sub>
		<i>Thermus</i> (99)	<i>Deinococcus-Thermus</i>	DQ324868	OC	O <sub>2</sub>
NGB-PS	Fe(OH) <sub>3</sub> 65–75 °C	<i>Thermocrinis</i> (99)	Aquificales	DQ324873	H <sub>2</sub> , S <sub>2</sub> O <sub>3</sub> , S <sup>0</sup>	O <sub>2</sub>
		<i>Thermus</i> (99)	<i>Deinococcus-Thermus</i>	DQ324885	OC, As <sup>III</sup> ?	O <sub>2</sub>
		<i>Thermomicrobium</i> (99)	Chloroflexi	DQ324896	OC, As <sup>III</sup> ?	O <sub>2</sub>

\*16S rRNA sequences from ASC springs in NGB were compiled from Jackson *et al.* (2001), Inskeep *et al.* (2004) and Macur *et al.* (2004a).

<sup>†</sup>Major geochemical (e.g. dominant solid phase) and temperature zones at and down gradient of geothermal source.

<sup>‡</sup>Values in parentheses are the percentage similarity to nearest cultivated relatives in GenBank (Benson *et al.*, 2005). Sequences whose closest cultivated relatives are <93% are not discussed here.

<sup>§</sup>The exact stoichiometry of the stibnite-like, Sb-S phase is under study.

<sup>¶</sup>Primary studies are cited in text.

\*\*OC = organic carbon; As<sup>III</sup> ? = close relatives have been shown to oxidize As<sup>III</sup> but not necessarily for energy gain.

bacterial and archaeal 16S rRNA gene sequences were observed, but these were not closely related to known cultured relatives and are not presented here (W. P. Inskeep, unpublished data).

Several similar 16S rDNA sequences were observed in the acidic springs as a function of distance from geothermal dis-

charge. For example, *Stygiolobus*-like sequences have been detected in the near source water environments where dissolved O<sub>2</sub> levels are at or below detection. The reported metabolism of this organism suggests that it oxidizes H<sub>2</sub> using elemental S as an electron acceptor (Seeger *et al.*, 1991). If so, this organism is actually establishing a small S cycle

[between S(0) and S(-II)] after the formation of elemental S on the spring floor, regenerating dissolved sulfide. *Hydrogenobaculum*-like sequences are also common to both the acid-sulfate-chloride springs of Norris Basin and the acid-sulfate Rainbow Spring (RS2). In fact, numerous *Hydrogenobaculum*-like sequences are detected throughout the outflow channels in the acidic spring types (Macur *et al.*, 2004a; Table 4). In culture, these Aquificales are generally aerobic to microaerobic and may oxidize H<sub>2</sub>, S<sup>0</sup> and or As<sup>III</sup> using O<sub>2</sub> as an electron acceptor (Donahoe-Christiansen *et al.*, 2004; Reysenbach *et al.*, 2005). Consequently, these organisms will depend on variable fluxes of O<sub>2</sub> supplied via ingassing, and if oxidizing H<sub>2</sub> or S<sup>0</sup>, would likely be in their optimum habitat throughout the S<sup>0</sup> depositional zones.

As the acidic outflow channels become oxygenated and H<sub>2</sub>S levels decline to below 1–2 μM, Fe-oxide phases become the dominant solid phase. Much of the Fe biomineralization occurs as encrustations and sheaths around microbial filaments (Inskeep *et al.*, 2004; Macur *et al.*, 2004a). Pronounced changes in phylogeny occur in both acidic spring types including appearance of archaeal and bacterial sequences whose close relatives have all been implicated in the oxidation of Fe<sup>II</sup>. The presence of *Metallosphaera*, *Sulfobacillus*, *Acidimicrobium* and *Thiomonas*-like sequences in the Fe-oxide mats is generally consistent with possible chemolithotrophy on Fe<sup>II</sup> using O<sub>2</sub> as an electron acceptor (Peeples & Kelly, 1995; Norris *et al.*, 1996; Bruneel *et al.*, 2003; Johnson *et al.*, 2003). There is also evidence of heterotrophic populations that may reduce Fe<sup>III</sup> such as sequences related to Acetobacteraceae Y008, an isolate obtained from Norris Basin (Johnson *et al.*, 2003).

Comparison of 16S rDNA sequences obtained from the near-neutral springs reveals several important clues about geochemical factors controlling the types of micro-organisms found in these geothermal ecosystems. The presence of significant dissolved sulfide at higher pH and the subsequent slower disappearance rates of sulfide down gradient contribute to slower oxygenation. Within the source pool and adjacent sediments, predominant sequence types observed were highly related to *Geothermobacterium ferrireducens*, an organism capable of oxidizing H<sub>2</sub> with Fe<sup>III</sup> as an electron acceptor (Kashefi *et al.*, 2002), and a suite of chemoorganotrophic organisms that are likely reducing elemental S using organic C (OC) as an electron donor (e.g. *Vulcanisaeta*, *Caldococcus*, *Thermofilum*; Kjems *et al.*, 1990; Aoshima *et al.*, 1996; Itoh *et al.*, 2002). Below temperatures of 70 °C, *Thermocrinus* and *Sulfurihydrogenibium*-like sequences become important. In culture, these Aquificales require H<sub>2</sub>, S<sup>0</sup>, S<sub>2</sub>O<sub>3</sub> or Fe<sup>II</sup> for growth under aerobic to microaerobic conditions (Huber *et al.*, 1998; Aguiar *et al.*, 2004). Consequently, although O<sub>2</sub> ingassing is considerably slower in JC3, these organisms require some flux of O<sub>2</sub> and are not observed in the source pool sediments. Interestingly, the sequence data from JC3 suggest that microaerobic to aerobic Aquificales and anaerobic

S<sup>0</sup>-reducing organisms such as *Desulfurella* and *Caldisphaera* (Miroshnichenko *et al.*, 1998; Itoh *et al.*, 2003) are both important groups of organisms down gradient; this is consistent with the minimal oxygenation occurring throughout the outflow channel of JC3.

Conversely, the near-neutral NGB-PS contains very little dissolved sulfide and the source waters appear partially oxygenated upon discharge (e.g. As<sup>V</sup>/As<sup>TS</sup> ratios are ~0.38 at source water discharge as compared to ~0.05–0.1 in the other systems; Fig. 4). *Thermocrinus* and *Thermus*-like sequences are the most dominant clones observed in NGB-PS (Table 4). Organisms represented by the *Thermocrinus*-like sequences may be oxidizing H<sub>2</sub> with O<sub>2</sub> as an electron acceptor (Huber *et al.*, 1998). Unlike the other springs, there were no sequences observed in NGB-PS that could be inferred through close relatives to be engaged in any kind of elemental S reduction, consistent with the direct observation that low dissolved sulfide values of <2–3 μM are not sufficient to deposit elemental S, and support subsequent S reducers. Interestingly, no obvious sequences were detected that could be used to support the assumption that Fe<sup>II</sup> chemotrophy is occurring in this system. The abiotic rates of Fe<sup>II</sup> oxidation to form Fe<sup>III</sup> oxides increase dramatically above pH values of 4.5 (Nordstrom & Southam, 1997); consequently, abiotic Fe oxidation may make a greater contribution to Fe<sup>III</sup>-oxide deposition than in the acidic springs where phylogenetic evidence strongly supports the presence of Fe<sup>II</sup>-oxidizing chemotrophs. The free-energy values for Fe oxidation are –65 to –75 kJ mol<sup>-1</sup> e<sup>-</sup> (e.g. Reactions 24, 25) in NGB-PS compared to only –25 to –30 kJ mol<sup>-1</sup> e<sup>-</sup> in the acidic systems. Consequently, reliance on the magnitude of free-energy values for Fe oxidation to infer population distribution is not entirely consistent with observed phylogeny. As temperatures in the outflow channel of NGB-PS cool to ~65 °C, *Thermomicrobium*-like sequences have been recovered. Cultivated *Thermomicrobium* sp. are aerobic heterotrophs of the Chloroflexi (Jackson *et al.*, 1973), some members of which can potentially oxidize As<sup>III</sup> via *aox*-like genes (LeBrun *et al.*, 2003).

#### Variation in free-energy values within outflow channels

Calculated free-energy values for several representative redox reactions are each poised within a fairly narrow energy window as a function of distance within the outflow channels (Fig. 5). This behaviour is essentially mirrored in the estimated electron activity values from various half-cell reactions (Fig. 3) down gradient in each spring and is controlled by the respective standard state free-energy values and a corresponding range of possible ratios of oxidized to reduced species. For example, there is no significant change in free-energy values (per mol electron) for H<sub>2</sub> oxidation, H<sub>2</sub>S oxidation or Fe<sup>II</sup> oxidation as a function of distance within the outflow channels that would assist in demarcating termination of S<sup>0</sup> deposition followed by deposition of Fe<sup>III</sup>-oxide like phases observed in the pH 2.5–3 springs (e.g. see Fig. 1; Table 3), or the striking As<sup>III</sup>

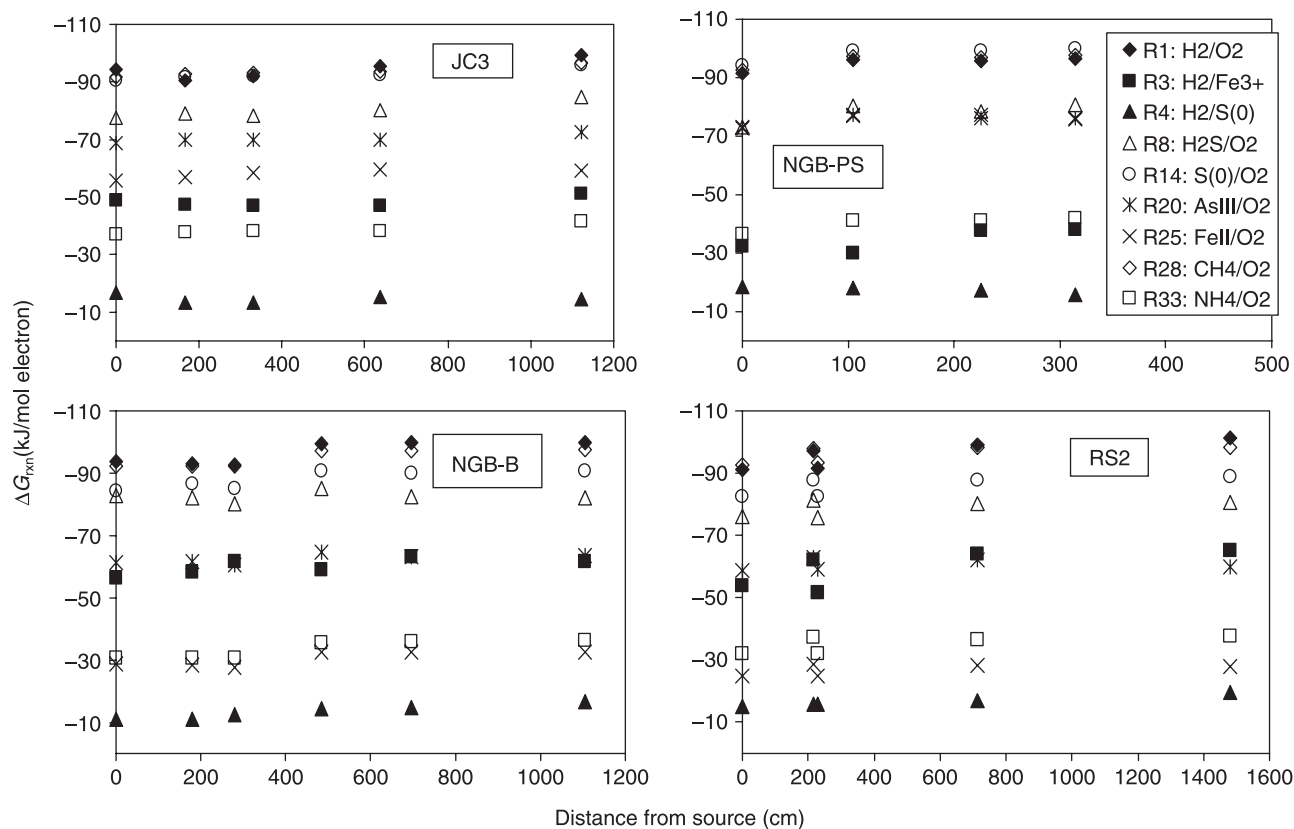


**Fig. 5** Calculated free-energy values ( $\Delta G_{\text{rxn}}$ , kJ/mole electron) for selected reactions (full reactions are given in Table 2) plotted as a function of distance within the outflow channels. Free-energy values for each reaction maintain a narrow range, despite variable conditions observed within the outflow channels that create steep gradients in geochemical conditions as a function of distance.

oxidation patterns observed in all springs that occur at well-defined positions based in part on the different amounts of dissolved oxygen and dissolved sulfide (Fig. 4). Although significant changes in geochemistry and phylogeny occur within outflow channels (Fig. 4, Table 4), the calculated free-energy values are not particularly sensitive to these changes and offer poor resolution for understanding geochemical and temperature gradients occurring down stream of source discharge. Moreover, although the variation in observed microbial populations down gradient (Table 4) appear to reflect changes in geochemistry and temperature, the free-energy values do not reveal significant changes with distance that would correlate with the distribution of micro-organisms.

## DISCUSSION

### Sensitivity analysis of free-energy calculations

Redox couples involving  $\text{H}_2$ ,  $\text{H}_2\text{S}$ ,  $\text{S}^0$ ,  $\text{Fe}^{2+}$ ,  $\text{H}_3\text{AsO}_3$ ,  $\text{CH}_4$  and  $\text{NH}_4$  as electron donors with  $\text{O}_2$  as the oxidant are all highly exergonic in the source waters of the springs studied. As  $\text{O}_2$  concentrations increase down gradient due to air–water gas exchange, reactions with  $\text{O}_2$  generally become slightly more

exergonic, but in some cases the activities of electron donor are declining simultaneously, such as with the degassing of  $\text{H}_2\text{S}(\text{aq})$ ,  $\text{H}_2(\text{aq})$  and  $\text{CH}_4(\text{aq})$ . The value of  $\Delta G_{\text{rxn}}$  for each couple is fairly insensitive to changes in the activity of  $\text{O}_2(\text{aq})$ , within the range of detectable  $\text{O}_2(\text{aq})$  to saturation at 0.16 atm  $\text{O}_2(\text{g})$  (e.g. 0.08–140  $\mu\text{M}$ , total pressure at YNP elevation is approximately 0.77 atm). Consequently, in the case of highly exergonic reactions with  $\text{O}_2$ , it is obvious that detailed analytical measurements of individual sites will not change the conclusion that these reactions may be important for chemolithotrophic micro-organisms. As pointed out in Fig. 6 (Reaction 1), whether one assumes  $10^{-3.7} \text{ M } \text{O}_2$  (e.g. saturation) or  $10^{-20} \text{ M } \text{O}_2$  (e.g. 10 orders of magnitude lower than a reasonable detection limit) will have little impact on the conclusion that the knall-gas reaction (Reaction 1) is highly exergonic. Interpretations regarding the importance of  $\text{H}_2$  as an electron donor for microbial metabolism in geothermal systems cannot be based solely on energetic calculations, because it is clear that the reaction will always be exergonic, provided  $\text{O}_2(\text{aq})$  and  $\text{H}_2(\text{aq})$  are greater than  $\sim 10^{-25} \text{ M}$  (Fig. 6, Reaction 1). Consequently, the fact that this reaction is highly exergonic regardless of position within the outflow channel should not be over interpreted as evidence that  $\text{H}_2$

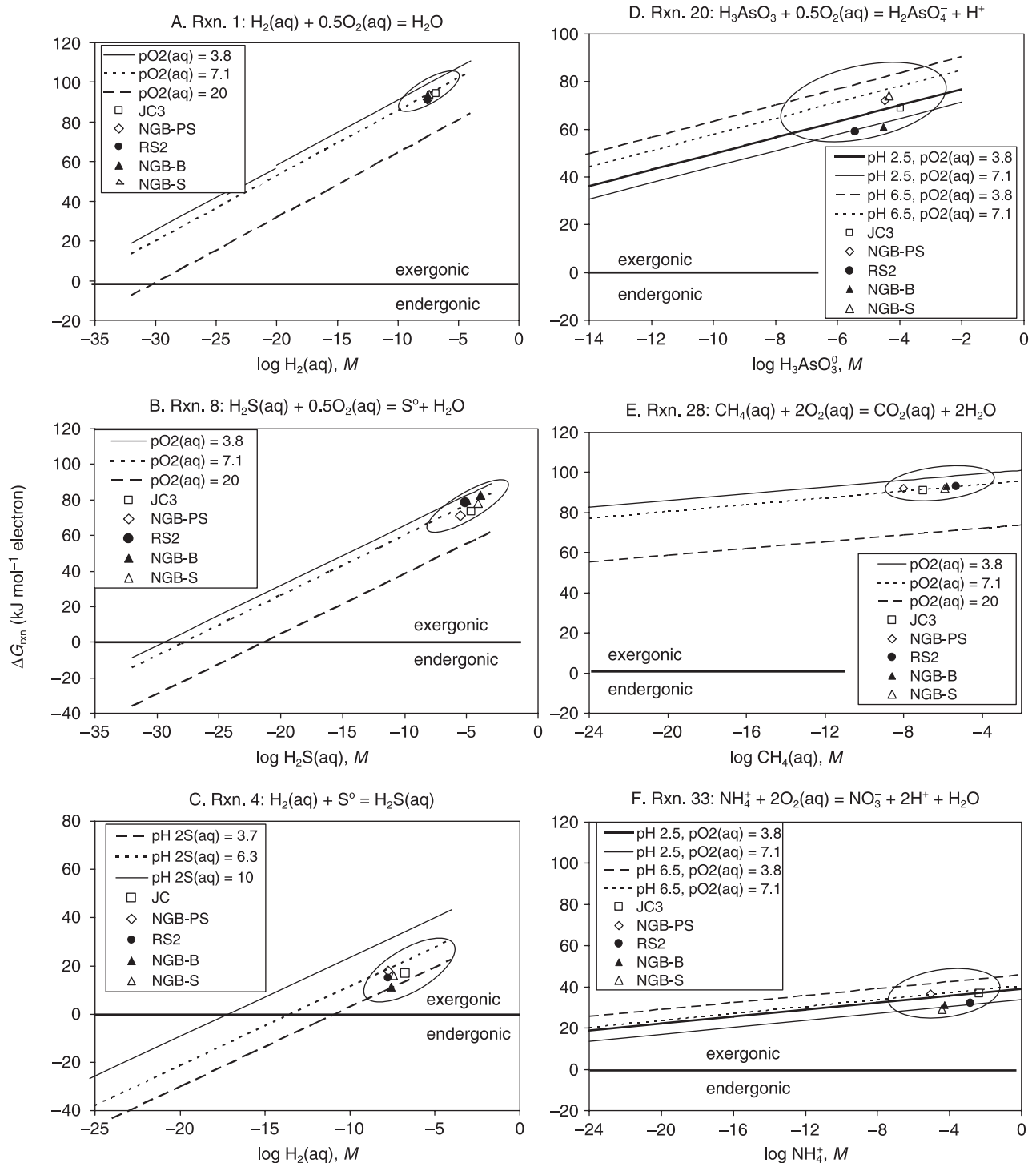


**Fig. 6** Sensitivity analysis of the dependence of free-energy values on reactant concentrations for several redox reactions (Reactions 1, 8, 4, 20, 28, 33; Table 2) that may be important for chemolithotrophic metabolism in geothermal springs. Circles represent estimated regions of the range in free-energy values corresponding to reactant detection limits or realistic upper concentration limits. Sensitivity analyses (lines) investigate ranges in pH, dissolved  $\text{O}_2$  and dissolved  $\text{H}_2\text{S}$  ( $p = -\log$ ). Results show that for most conditions experienced in natural systems, electron donor reactions with  $\text{O}_2(\text{aq})$  are highly exergonic and detailed chemical analyses of specific sites will not change this conclusion, given current detection limits.

oxidation is the dominant metabolism for all thermophiles across these geothermal gradients. Numerous thermophilic organisms (especially members of the Aquificales) may utilize the knall-gas reaction (Eder & Huber, 2002; Reysenbach *et al.*, 2005; Spear *et al.*, 2005a,b), but are likely confined to zones of higher  $H_2(aq)$  as defined by degassing rates (e.g. Figure 4). In fact, we have observed several 16S rRNA gene sequences within the higher  $H_2$  zones whose close relatives are known  $H_2$  oxidizers. These include *Hydrogenobaculum*-like sequences in ASC (NGB-B, NGB-S, NGB-D) and AS (RS2) springs (Shima & Suzuki, 1993) and *Sulfurihydrogenibium* and *Thermocrinis*-like sequences in near-neutral springs of JC3 and NGB-PS, respectively (Huber *et al.*, 1998; Aguiar *et al.*, 2004; Table 4). Many of the inferred  $H_2$ -oxidizing populations observed in the subject geothermal springs are microaerobic or aerobic organisms; consequently, some flux rate of  $O_2$  is necessary to support these populations *in situ*. The rates of  $O_2$  ingassing and aqueous  $O_2$  mass transfer are likely critical parameters for understanding the actual distribution of thermophiles that capitalize on the free energy available from  $O_2$  electron acceptor reactions. Phylogenetic evidence supports the assumption that  $H_2$  is an important electron donor, but not necessarily always with  $O_2$  as an electron acceptor, and not across all positions within the outflow channels (Table 4).

#### Sulfur oxidation

Reactions involving the oxidation of reduced S species by  $O_2(aq)$  are all highly exergonic in the systems considered (e.g. Reactions 8 [ $H_2S/S^0$ ], 9 [ $H_2S/SO_4^{2-}$ ] and 14 [ $S^0/SO_4^{2-}$ ]; Fig. 2). Again, this is not particularly surprising considering the standard state  $\Delta G_{rxn}^\circ$  values for these electron transfer reactions. Figure 6(B) identifies the plausible range of calculated  $\Delta G_{rxn}$  values for the oxidation of  $H_2S$  via  $O_2$  (Reaction 8) and indicates that irrespective of the amounts of  $H_2S$  or  $O_2$  measured (within detection), this reaction will be highly exergonic. Indeed,  $\Delta G_{rxn}$  values for each spring fall within the detection-saturation window shown in Fig. 6(B). It is important to question the utility of this result realizing that all systems will yield similar exergonic values for this redox couple. Several close relatives of 16S rDNA sequences obtained from within the  $H_2S$  degassing zone (Fig. 4) of the acidic springs (e.g. NGB-S and RS2) are known  $H_2S$  and or  $S^0$  oxidizers (Table 4). For example, *Hydrogenobaculum*-like populations are commonly observed, while *Sulfurihydrogenibium*-like populations appear in the higher pH spring JC3. Both genera are represented by cultured organisms capable of oxidizing reduced S species (Shima & Suzuki, 1993; Reysenbach *et al.*, 2005). Given that several members of the Aquificales have been shown to be capable of oxidizing reduced S and or  $H_2$ , it is difficult to use energetic favourability as an argument for which metabolism is most important in the near source water environments of sulfidic geothermal springs.

#### Sulfur reduction

The oxidation of  $H_2$  with  $S^0$  as the electron acceptor (Reaction 4) is an interesting redox couple to consider further, especially given that it represents one of the most primitive possible chemolithotrophic processes in the absence of  $O_2$ . Energetic analyses (Fig. 6C) show that this reaction is significantly less exergonic than many other possible reactions with  $O_2$  as an electron acceptor, yielding values of only  $-10$  to  $-20$  kJ mol<sup>-1</sup> electron, near the potential limits of minimum energy requirements to support cellular metabolism (Hoehler *et al.*, 2001; Jackson & McInerney, 2002). The plausible window of  $\Delta G_{rxn}$  values shows that this reaction will generally be exergonic, although only down to  $H_2(aq)$  activities of  $10^{-10}$ – $10^{-12}$  M at high  $H_2S$  (e.g. mM levels). Do the lower values of  $\Delta G_{rxn}$  suggest that this reaction is less important for chemolithotrophs and that this will not be a preferred metabolism in these systems? Phylogenetic analyses of the springs studied indicate that *Stygiolobus*, *Caldococcus*, *Vulcanisaeta* and *Caldisphaera*-like sequences (Table 4) are important populations observed in the  $S^0$  depositional zones of all springs studied with the exception of NGB-PS, which contains dissolved sulfide values  $<3$   $\mu$ M. Cultivated relatives of these sequences are known to utilize  $S^0$  as an electron acceptor via either  $H_2$  (*Stygiolobus azoricus*; Segerer *et al.*, 1991) or organic C (*Vulcanisaeta*, *Caldococcus*, *Caldisphaera* sp.; Aoshima *et al.*, 1996; Itoh *et al.*, 2002; Itoh *et al.*, 2003) as electron donors. Consequently, despite the lower  $\Delta G_{rxn}$  values for the reduction of elemental  $S^0$  via  $H_2$  (Reaction 4), this reaction may be quite important in supporting anaerobic primary producers. Free-energy values for organotrophic reduction of elemental S are also estimated to be low ( $-25$  to  $-35$  kJ mol<sup>-1</sup> e<sup>-</sup>; data not shown) relative to other highly exergonic reactions. In all springs studied, where present, these populations were confined to the near-source water zones prior to significant  $O_2$  ingassing, and where  $S^0$  was ubiquitous along the channel floor. Consequently, although steep gradients in dissolved  $H_2S$  and  $H_2$  are important in defining specific niches within the outflow channel, the importance of anaerobic S reducers would have been difficult to predict based solely on the magnitude of calculated free-energy values (e.g. Figures 2 and 6).

#### Arsenic oxidation

The oxidation of  $H_3AsO_3^{\ominus}$  with  $O_2$  is also highly exergonic ( $-50$  to  $-80$  kJ mol<sup>-1</sup> electron), independent of dissolved  $O_2$  concentrations ranging from detection to saturation (Fig. 6D). Rapid oxidation rates of As<sup>III</sup> are observed in all springs studied (Fig. 4), and this has been shown to be mediated by micro-organisms in several of the ASC springs (Langner *et al.*, 2001; Macur *et al.*, 2004a), and in other geothermal watersheds (Wilkie & Hering, 1998; Gihring *et al.*, 2001). However, the actual mechanisms and dynamics of microbial As<sup>III</sup> oxidation are not well understood and may

or may not be related to chemolithotrophic metabolism (e.g. see reviews by Silver & Phung, 2005; Cervantes *et al.*, 1994; Mukhopadhyay *et al.*, 2002; Oremland & Stolz, 2003). Definitive chemolithotrophic metabolism on As<sup>III</sup> has only been reported for several micro-organisms (Santini *et al.*, 2000, 2002; Oremland *et al.*, 2002; Bruneel, 2004), yet detoxification strategies involving *aox*-like genes may also contribute to observed As<sup>III</sup> oxidation (LeBrun *et al.*, 2003; Muller *et al.*, 2003; Macur *et al.*, 2004b; Silver & Phung, 2005). Dissolved sulfide (H<sub>2</sub>S(aq)) has been shown to inhibit As<sup>III</sup> oxidation in *Hydrogenobaculum*-like populations (Donahoe-Christiansen *et al.*, 2004) and this observation is consistent with As speciation profiles in ASC springs (e.g. NGB-B; Fig. 4) where As<sup>III</sup> oxidation commences after dissolved sulfide concentrations drop below ~2 μM. However, in the near-neutral JC3 thermal spring, As<sup>III</sup> oxidation occurs despite the presence of total dissolved sulfide ranging from 15 to 30 μM within the outflow channel. At this time, it is not known whether organisms within these springs are oxidizing As<sup>III</sup> for energy gain, but it is clear that the dynamics of As speciation within the geothermal outflow channels are controlled by a combination of biotic and abiotic factors that cannot be resolved through general examination of free-energy values. Microbial detoxification pathways, which often have a significant impact on trace element cycling in natural systems, generally require energy (Rosen, 2002); consequently, the energetic favourability of a particular inorganic couple may not be of immediate value for understanding microbial-geochemical linkages.

The oxidation of CH<sub>4</sub> to CO<sub>2</sub> (methanotrophy) and NH<sub>4</sub><sup>+</sup> to NO<sub>3</sub><sup>-</sup> (nitrification) are also considerably exergonic under all plausible conditions (Fig. 6E,F). The free-energy values are poised from approximately -80 to -100 kJ mol<sup>-1</sup> electron for the oxidation of CH<sub>4</sub> via O<sub>2</sub>, and from -20 to -40 kJ mol<sup>-1</sup> electron for the oxidation of NH<sub>4</sub><sup>+</sup> via O<sub>2</sub> (Fig. 6E,F). The acidic geothermal springs (NGB-B, S and RS2) and the near-neutral JC3 spring contain significant quantities of CH<sub>4</sub>(aq) in the source waters (Table 1). However, it is not clear from phylogenetic analyses whether there are organisms within these springs that may be utilizing CH<sub>4</sub>(aq) as an electron donor. To date, none of the 16S rDNA sequences identified in these springs have obvious cultivated relatives known to oxidize CH<sub>4</sub> (Jackson *et al.*, 2001; Macur *et al.*, 2004a; S. Korf, unpublished data). Certainly, it is possible that micro-organisms represented by 16S rDNA sequences with poor matches to cultivated relatives may be involved in CH<sub>4</sub> oxidation. However, methane oxidation may be inhibited in highly acidic conditions (Hanson & Hanson, 1996). Consequently, until we understand the physiology and activity of relevant microbial populations in these systems, it is not possible to conclude that CH<sub>4</sub> is an important electron donor, despite the fact that it is one of the most exergonic processes possible. Similarly, the oxidation of NH<sub>4</sub><sup>+</sup> to NO<sub>3</sub><sup>-</sup> is highly exergonic; however, this reaction may not be important to chemolithotrophs in acidic

geothermal systems (Kowalchuk & Stephen, 2001), despite the fact that concentrations of NH<sub>4</sub> are 1.7 and 5.5 mM in RS2 and JC3, respectively. No consumption of NH<sub>4</sub><sup>+</sup> or production of NO<sub>3</sub><sup>-</sup> (or NO<sub>2</sub><sup>-</sup>) has been observed throughout the outflow channels of the springs studied (data not shown), suggesting little microbial oxidation of NH<sub>4</sub> is occurring despite the fact that it is highly exergonic.

#### Reactions with Iron

Redox reactions involving Fe<sup>II</sup> as an electron donor or Fe<sup>III</sup> as an electron acceptor are particularly important in YNP geothermal springs (e.g. Reactions 3, 12, 22, 24–27, Table 3), and of all the redox reactions considered, free-energy values of reactions involving Fe are the most variable across sites. Moreover, due to the nonequilibrium nature of these systems, both the oxidation of Fe<sup>II</sup> and the reduction of Fe<sup>III</sup> are exergonic in all the geothermal systems considered here (e.g. reactions 24 and 25 and 3, 12, 17 and 18 in Table 2). Given these divergent thermodynamic possibilities, factors other than the calculated thermodynamic favourability play an important role in defining the fate of Fe in these systems and explain the biomineralization of Fe<sup>III</sup> oxides observed in NGB-B, NGB-S and NGB-PS compared to the formation of FeS<sub>2</sub> in JC3. In the current study, we examined two general situations: (i) low pH geothermal springs containing high aqueous Fe<sup>II</sup> ranging from 0.05 to 0.1 mM (NGB-B, NGB-S, RS2), or (ii) near-neutral pH springs (NGB-PS, JC3) containing less than 2 μM aqueous Fe. In the acidic springs, Fe<sup>II</sup> is the dominant valence state at the source (>98% Fe<sup>II</sup>) and no consistent losses of dissolved Fe are observed down gradient, indicating that the flux of total soluble Fe is high relative to the accumulation rate of Fe<sup>III</sup> solid phases within the outflow channel (Langner *et al.*, 2001). The amounts of Fe<sup>II</sup> and Fe<sup>III</sup> in JC3 and NGB-PS are more difficult to assess at less than 2 μM total Fe, but we have consistently observed a mixture of Fe<sup>II</sup> and Fe<sup>III</sup> in the source waters of these springs. The corresponding energetic analyses for all four geothermal springs show that oxidation reactions of Fe<sup>II</sup> with O<sub>2</sub> are exergonic (range of -20 to -70 kJ mol<sup>-1</sup> electron) either written as a reaction to form soluble Fe<sup>3+</sup> (Reaction 24) or to form Fe<sup>III</sup>-oxides such as ferrihydrite (Fe(OH)<sub>3</sub>) (Reaction 25). Simultaneously, the reduction of Fe<sup>3+</sup> with H<sub>2</sub>(aq) (Reaction 3) is favourable in these geothermal springs, and free-energy values also range from ~-25 to -50 kJ mol<sup>-1</sup> electron (Fig. 7C). Consequently, without additional knowledge of the processes actually occurring and the microbial populations actually inhabiting these sites, energetic approaches are of limited use for predicting dominant microbial processes involving Fe in these habitats.

When the actual processes and microbial populations are examined, it is clear that Fe<sup>II</sup> oxidation is very important in the acidic springs, where copious amounts of Fe(OH)<sub>3</sub> phases (and jarosite in RS2) are formed due to microbial processes (Inskeep *et al.*, 2004; Macur *et al.*, 2004a). Several of the microbial populations identified in the Fe mats of NGB-B,

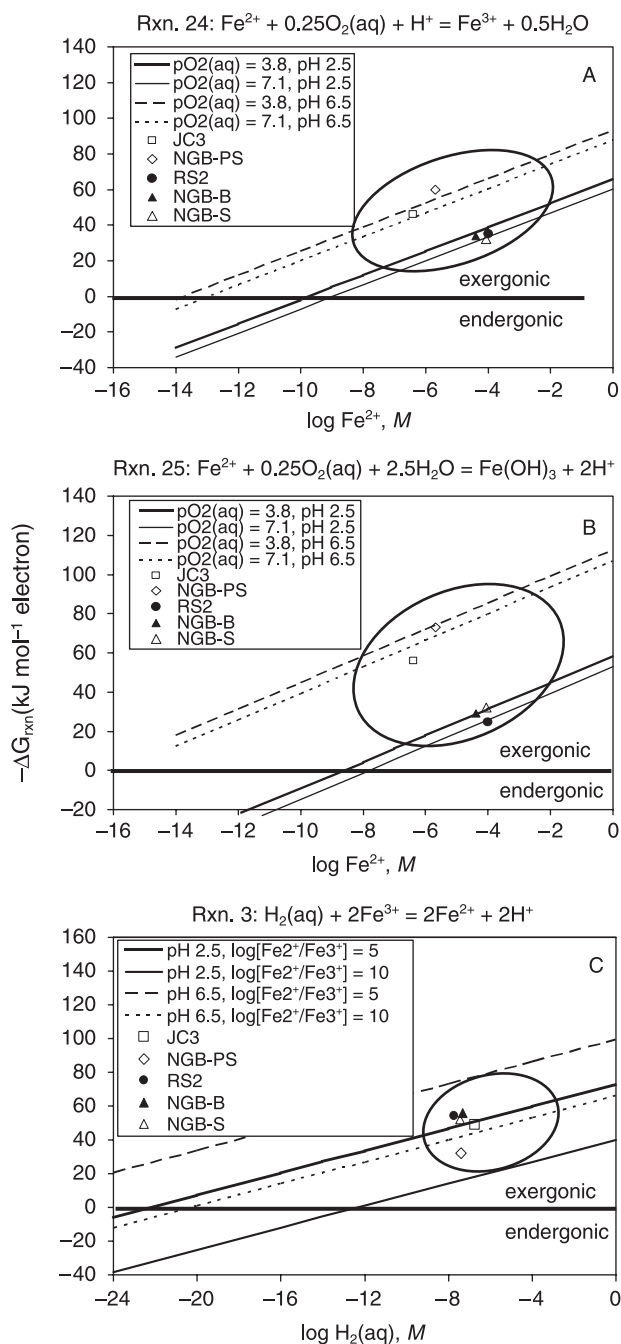


**Fig. 7** Sensitivity analysis of the dependence of free-energy values on reactant concentrations [ $\text{pO}_2(\text{aq}) = -\log(\text{O}_2, \text{aq})$ ] for several redox reactions involving either  $\text{Fe}^{2+}$  as an electron donor (A, B) or  $\text{Fe}^{3+}$  as an electron acceptor (C). Note that in most cases where  $\text{Fe}^{2+}$ ,  $\text{Fe}^{3+}$  and  $\text{H}_2(\text{aq})$  are detectable, reactions 3, 24 and 25 (Table 2) are all exergonic, but free-energy values are more variable due to reaction pH dependence as well as variation in  $\text{Fe}^{3+}$  activity with pH.

NGB-S and RS2 via 16S rDNA sequence analysis are closely related to known  $\text{Fe}^{\text{II}}$ -oxidizing organisms including *Metallosphaera*, *Acidimicrobium*, *Sulfobacillus* and *Thiomonas* (Table 4) (Fuchs *et al.*, 1995; Peeples & Kelly, 1995; Norris *et al.*, 1996; Bruneel *et al.*, 2003; Johnson *et al.*, 2003). The

higher pH springs (JC3 and NGB-PS) clearly show higher free-energy values for  $\text{Fe}^{2+}$  oxidation due to significant decreases in  $\text{H}^+$  activity (Reaction 25), or the lower calculated  $\text{Fe}^{3+}$  activities (Reaction 24) (Fig. 7A,B). The oxidation of  $\text{Fe}^{\text{II}}$  in NGB-PS has not yet been linked to potential  $\text{Fe}^{\text{II}}$  oxidizing populations, and may represent a greater contribution from the more rapid chemical rate of  $\text{Fe}^{\text{II}}$  oxidation above pH 4.5 (Nordstrom & Southam, 1997). Conversely, no  $\text{Fe}^{\text{II}}$  oxidation is observed throughout the outflow channel of JC3. In fact, pyrite ( $\text{FeS}_2$ ) is a dominant solid phase formed in the source pool and is also found distributed down gradient. Phylogenetic analyses (16S rDNA) of sediments taken from JC3 indicate that *G. ferrireducens*-like organisms are likely the predominant bacteria inhabiting the source pool sediments (Table 4). The metabolism reported for the anaerobic *G. ferrireducens* involves  $\text{H}_2$  oxidation via  $\text{Fe}^{3+}$  as an electron acceptor (Kashefi *et al.*, 2002), and this is consistent with the formation of  $\text{FeS}_2$  in this particular spring.

Although the energetic analyses show that both  $\text{Fe}^{\text{II}}$  oxidation and  $\text{Fe}^{\text{III}}$  reduction are exergonic in all springs studied, the dominant processes result in either the formation of  $\text{Fe}^{\text{III}}$ -oxide solid phases or the  $\text{Fe}^{\text{II}}$ -sulfide solid phases. The major factor that appears to control the fate of Fe is the rate of dissolved sulfide degassing and the inversely correlated rate of  $\text{O}_2$  ingassing (Fig. 4). In the acidic springs, degassing of dissolved sulfide is encouraged due to the fact that  $\text{H}_2\text{S}(\text{aq})$  is the dominant species of dissolved sulfide at low pH (<5), and  $\text{Fe}^{\text{II}}$  oxidation commences as soon as dissolved sulfide levels drop to below 1–2  $\mu\text{M}$ . Conversely, the rate of sulfide degassing is much slower in JC3 due to the fact that  $\text{HS}^-$  is a more important soluble species of dissolved sulfide. The oxidation of  $\text{Fe}^{2+}$  is likely limited by insufficient  $\text{O}_2$  mass transfer, and the slower degassing rates of dissolved sulfide encourages the formation of  $\text{Fe}^{\text{II}}$ -sulfide solid phases (Luther *et al.*, 2003). Consequently, the processes that appear to be most important in defining the geochemical and microbial community trajectory are related to rates of air–water gas exchange.

### Energy fluxes and kinetics in dynamic environments

How might we improve the utility of energetic analyses for understanding the role of biota in geochemical cycling? One possibility would be to express the energy available to microorganisms as an energy flux in units of energy per unit area per unit time (e.g.  $\text{kJ m}^{-2} \text{min}^{-1}$ ). Although the velocity ( $\text{m min}^{-1}$ ) at any single point within a watershed or geothermal outflow channel will be a constant scalar for all reactions considered, the actual concentrations of various electron donors will vary and modify the energy flux. Consequently, rather than considering the energy available per mole of electron, the energy flux provides an additional and perhaps more meaningful estimate of the energy available to microorganisms at a given location in the flowing channel. Energy fluxes can be calculated based on concentrations of either the

electron donor or the electron acceptor at specific points within the outflow channels. For example, energy fluxes were calculated for source-water conditions in NGB-B based on concentrations of electron donors including  $\text{H}_2$ ,  $\text{H}_2\text{S}$ ,  $\text{As}^{\text{III}}$ ,  $\text{NH}_4$  and  $\text{CH}_4$  and a measured velocity of approximately  $5 \text{ m min}^{-1}$ . Resultant energy fluxes range from  $0.007$  to  $0.02 \text{ kJ m}^{-2} \text{ min}^{-1}$  for reactions where  $\text{H}_2$  is an electron donor to values of  $30\text{--}500 \text{ kJ m}^{-2} \text{ min}^{-1}$  for reactions with  $\text{H}_2\text{S}$ ,  $5\text{--}15 \text{ kJ m}^{-2} \text{ min}^{-1}$  for reactions with  $\text{As}^{\text{III}}$ ,  $0.4\text{--}7 \text{ kJ m}^{-2} \text{ min}^{-1}$  for reactions with  $\text{Fe}^{\text{II}}$ , and  $0.7\text{--}3 \text{ kJ m}^{-2} \text{ min}^{-1}$  for reactions with  $\text{CH}_4$ . These calculations show that although  $\text{H}_2$  oxidation is highly exergonic per mole electron transferred, the potential energy flux based on the actual concentration of  $\text{H}_2$  is fairly low compared to the energy flux from other electron donors. The reactions with  $\text{H}_2\text{S}$  as an electron donor yield the greatest energy fluxes due to the higher concentration of  $\text{H}_2\text{S}$  relative to other potential electron donors, and the energy fluxes for reactions where  $\text{CH}_4$ ,  $\text{Fe}^{\text{II}}$  and  $\text{As}^{\text{III}}$  serve as electron donors are one to two orders of magnitude greater than reactions with  $\text{H}_2$ . Despite the lower energy flux for reactions with  $\text{H}_2$ , phylogenetic analyses of the ASC springs (Jackson *et al.*, 2001; Macur *et al.*, 2004a) suggest that  $\text{H}_2$  is likely an important electron donor, especially near the point of spring discharge, prior to significant degassing. Phylogenetic analyses and subsequent physiological inference of other near-neutral geothermal systems in YNP also suggest that  $\text{H}_2$  is an important electron donor driving primary productivity (Shock *et al.*, 2005; Spear *et al.*, 2005a,b). However, it is incorrect to assume that  $\text{H}_2$  is the only important electron donor in the source pools and especially the outflow channels of geothermal springs.

Although energy fluxes may be an additional approach for understanding the distribution of microbial populations in geothermal systems, they too will be limited in their ability to predict the distribution of microbial populations, in part due to the steep gradients in concentrations of dissolved gases and in part due to the physiological realities of adapted microbial populations. A complete understanding of geochemical-microbial interactions in geothermal systems will require integration of biotic and abiotic processes in a dynamic framework that includes relevant reaction rates coupled with the activities of relevant microbial populations (Inskeep & McDermott, 2005). In this regard, future studies will continue to identify the dominant community members in model geothermal systems and characterize their physiological attributes. Moreover, knowledge of the expression of particular functional genes in these chemotrophic environments would be extremely beneficial for testing hypotheses regarding the primary electron donors and acceptors responsible for primary productivity (Newman & Banfield, 2002).

It is clear that the actual distribution of adapted microbial populations and their respective activities are correlated with geochemical conditions, but it is not necessarily clear which abiotic geochemical processes may be the most

important in actually controlling the distribution and activity of a specific micro-organism. Certainly, temperature and pH are important parameters that may directly impact microbial community structure. Indirectly, pH can have an enormous impact on other geochemical processes that may have a global impact on geochemical conditions and resultant phylogeny, such as the slower degassing rates of  $\text{H}_2\text{S}$  in JC3. Air-water exchange reactions are responsible for significant chemical mass transfer across the air-water interface over very short distances (cm to m). Consequently, steep gradients in dissolved  $\text{O}_2$  and other gases play an important role in defining the distribution of microbial populations and changes in aqueous and solid phase geochemistry occurring down gradient of thermal discharge. Physical factors such as velocity, air-water surface area and turbulence link directly to rates of air-water gas exchange, and these same processes control rates of temperature decline in geothermal outflow channels. Further phylogenetic analyses coupled with functional gene analysis and measurements of gene expression (Croal *et al.*, 2004) may clarify the importance of gas exchange rates in defining the distribution of microbial populations in geothermal systems. An integration of abiotic and biotic reaction rates controlling geochemical processes could lead to the development of more comprehensive kinetic models (e.g. Wang & van Cappellen, 1996; Mayer *et al.*, 2002) that recognize the importance of key abiotic reactions as well as microbial activities of specific adapted populations. Although energetic analyses can tell us what is possible, it is clear that our understanding of biogeochemical cycling and geobiology is predicated on the paths and actual rates of specific processes. Moreover, interpretations regarding the comparison of numerous free-energy values for redox couples across different sites must be tempered with the reality that the standard state free-energy value for a chosen redox reaction poises the reaction within a relatively narrow range of free-energy values, especially when activities of both oxidized and reduced species are above analytical detection limits.

## ACKNOWLEDGEMENTS

The authors appreciate support for this research from the Thermal Biology Institute (NASA Projects NAG5-8807 and NNG04GR46G), the National Science Foundation Microbial Observatory Program (MCB-0132022), and the Montana Agricultural Experiment Station (Project 911398). This work would not have been possible without permission from the Yellowstone National Park Center for Resources and the generous assistance of J. Varley, C. Hendrix, and A. Rodman.

## REFERENCES

- Aguiar P, Beveridge TJ, Reysenbach AL (2004) *Sulfurihydrogenibium azorense*, sp. nov., a thermophilic hydrogen-oxidizing

- microaerophile from terrestrial hot springs in the Azores. *International Journal of Systematic and Evolutionary Microbiology* **54**, 33–39.
- Allison JD, Brown DS, Novo-Gradac KJ (1991) MINTEQA2/PRODEFA2, a geochemical assessment model for environmental systems: Version 3.0 User's Manual. Environmental Research Laboratory, Office of Research and Development, USEPA, Athens, Georgia.
- Amend JP, Rogers KL, Shock EL, Gurreri S, Inguaggiato S (2003) Energetics of chemolithotrophy in the hydrothermal system of Vulcano Island, southern Italy. *Geobiology* **1**, 37–58.
- Amend JP, Shock EL (2001) Energetics of overall metabolic reactions of thermophilic and hyperthermophilic Archaea and Bacteria. *FEMS Microbiology Reviews* **25**, 175–243.
- Aoshima M, Nishibe Y, Hasegawa M, Yamagishi A, Oshima T (1996) Cloning and sequencing of a gene encoding 16S ribosomal RNA from a novel hyperthermophilic archaeobacterium NC12. *Gene* **180**, 183–187.
- APHA (1998) *Standard Methods for the Examination of Water and Wastewater* (eds Clesceri, LS, Greenberg, AE, Eaton, AD). American Public Health Association, Washington, D.C.
- Ball JW, McCleskey RB, Nordstrom DK, Holloway JM, Verplanck PL (2002) Water-chemistry data for selected springs, geysers, and streams in Yellowstone National Park, Wyoming 1999–2000. United States Geological Survey Open File Report 02-382, Boulder, Colorado.
- Benson DA, Karsch-Mizrachi I, Lipman DJ, Ostell J, Wheeler DL (2005) GenBank. *Nucleic Acids Research* **33**, D34–D38.
- Bruneel O (2004) *Contribution to the study of the geochemical and bacteriological mechanisms in the transport of mining pollution at the site of Carnoulès (Gard, France)*. PhD Thesis, University Montpellier II, France.
- Bruneel O, Personné JC, Casiot C, Leblanc M, Elbaz-Poulichet F, Mahler BJ, Le Flèche A, Grimont PAD (2003) Mediation of arsenic oxidation by *Thiomonas* sp. in acid-mine drainage (Carnoulès, France). *Journal of Applied Microbiology* **95**, 492–499.
- Cervantes C, Ji G, Ramirez JL, Silver S (1994) Resistance to arsenic compounds in microorganisms. *FEMS Microbiology Reviews* **15**, 355–367.
- Choi J, Hulseapple SM, Conklin MH, Harvey JW (1998) Modeling CO<sub>2</sub> degassing and pH in a stream-aquifer system. *Journal of Hydrology* **209**, 297–310.
- Croal LR, Gralnick JA, Malasarn D, Newman DK (2004) The genetics of geochemistry. *Annual Reviews of Genetics* **38**, 175–202.
- Davis CC, Knocke WR, Edwards M (2001) Implications of aqueous silica sorption to iron hydroxide: mobilization of iron colloids and interference with sorption of arsenate and humic substances. *Environmental Science and Technology* **35**, 3158–3162.
- Donahoe-Christiansen J, D'Imperio S, Jackson CR, Inskeep WP, McDermott TR (2004) Arsenite-oxidizing *Hydrogenobaculum* strain isolated from an acid-sulfate-chloride geothermal spring in Yellowstone National Park. *Applied and Environmental Microbiology* **70**, 1865–1868.
- Eder W, Huber R (2002) New isolates and physiological properties of the *Aquificales* and description of *Thermocrinis albus* sp. nov. *Extremophiles* **6**, 309–318.
- Fournier RO (1989) Geochemistry and dynamics of the Yellowstone National Park hydrothermal system. *Annual Review of Earth and Planetary Science* **17**, 13–53.
- Fuchs T, Huber H, Teiner K, Burggraf S, Stetter KO (1995) *Metallosphaera prunae* sp. nov., a novel metal-mobilizing, thermoacidophilic *Archaeum*, isolates from a uranium mine in Germany. *Systematic and Applied Microbiology* **18**, 560–566.
- Gihring TM, Druschel GK, McCleskey RB, Hamers RJ, Banfield JF (2001) Rapid arsenite oxidation by *Thermus aquaticus* and *Thermus thermophilus*: field and laboratory investigations. *Environmental Science and Technology* **35**, 3857–3862.
- Hanson RS, Hanson TE (1996) Methanotrophic bacteria. *Microbiological Reviews* **60**, 439–471.
- Hoehler TM, Alperin MJ, Albert DB, Martens CS (2001) Apparent minimum free energy requirements for methanogenic Archaea and sulfate-reducing bacteria in an anoxic marine sediment. *FEMS Microbiology Ecology* **38**, 33–41.
- Huber R, Eder W, Heldwein S, Wanner G, Huber H, Rachel R, Stetter KO (1998) *Thermocrinis ruber* gen. nov., sp. nov., a pink-filament forming hyperthermophilic bacterium isolated from Yellowstone National Park. *Applied and Environmental Microbiology* **64**, 3576–3583.
- Inskeep WP, Macur RE, Harrison G, Bostick BC, Fendorf S (2004) Biomineralization of As(V)-hydrous ferric oxyhydroxide in microbial mats of an acid-sulfate-chloride geothermal spring, Yellowstone National Park. *Geochimica et Cosmochimica Acta* **68**, 3141–3155.
- Inskeep WP, McDermott TR (2005) Geomicrobiology of acid-sulfate-chloride springs in Yellowstone National Park. In *Geothermal Biology and Geochemistry of Yellowstone National Park* (eds Inskeep WP, McDermott TR). Thermal Biology Institute, Montana State University, Bozeman, Montana, pp. 143–162.
- Itoh T, Suzuki K, Nakase T (2002) *Vulcanisaeta distributa* gen. nov., sp. nov., and *Vulcanisaeta souniana* sp. nov., novel hyperthermophilic, rod-shaped crenarchaeotes isolated from hot springs in Japan. *International Journal of Systematic and Evolutionary Microbiology* **52**, 1097–1104.
- Itoh T, Suzuki K, Sanchez PC, Nakase T (2003) *Caldisphaera lagunensis* gen. nov., sp. nov., a novel thermoacidophilic crenarchaeote isolated from a hot spring at Mt. Maquiling, Philippines. *International Journal of Systematic and Evolutionary Microbiology* **53**, 1149–1154.
- Jackson CR, Langner HW, Donahoe-Christiansen J, Inskeep WP, McDermott TR (2001) Molecular analysis of microbial community structure in an arsenite-oxidizing acidic thermal spring. *Environmental Microbiology* **3**, 532–542.
- Jackson BE, McInerney MJ (2002) Anaerobic microbial metabolism can proceed close to thermodynamic limits. *Nature* **415**, 454–456.
- Jackson TJ, Ramaley RF, Meinschein WG (1973) *Thermomicrobium*, a new genus of extremely thermophilic bacteria. *International Journal of Systematic Bacteriology* **23**, 28–36.
- Jähne B, Haussbecker H (1998) Air-water gas exchange. *Annual Reviews of Fluid Mechanics* **30**, 443–468.
- Johnson DB, Okibe N, Roberto FF (2003) Novel thermoacidophilic bacteria isolated from geothermal sites in Yellowstone National Park: Physiological and phylogenetic characteristics. *Archives of Microbiology* **180**, 60–68.
- Kashefi K, Holmes DE, Reysenbach AL, Lovley DR (2002) Use of Fe(III) as an electron acceptor to recover previously uncultured hyperthermophiles: Isolation and characterization of *Geothermobacterium ferrireducens* gen. nov., sp. nov. *Applied and Environmental Microbiology* **68**, 1735–1742.
- Kjems J, Leffers H, Olesen T, Ingelore H, Garrett RA (1990) Sequence, organization and transcription of the ribosomal RNA operon and the downstream tRNA and protein genes in the archaeobacterium *Thermofilum pendens*. *Systematic and Applied Microbiology* **13**, 117–127.

- Kowalchuk GA, Stephen JR (2001) Ammonia-oxidizing bacteria: a model for molecular microbial ecology. *Annual Reviews of Microbiology* **55**, 485–529.
- Langner HW, Jackson CR, McDermott TR, Inskeep WP (2001) Rapid oxidation of arsenite in a hot spring ecosystem, Yellowstone National Park. *Environmental Science and Technology* **35**, 3302–3309.
- Lebrun E, Brugna M, Baymann F, Muller D, Lièvreumont D, Lett MC, Nitschke W (2003) Arsenite oxidase, an ancient bioenergetic enzyme. *Molecular Biology and Evolution* **20**, 686–693.
- Luther GW III, Glazer B, Ma S, Trouwborst R, Shultz BR, Druschel G, Kraiya C (2003) Iron and sulfur chemistry in a stratified lake: Evidence for iron-rich sulfide complexes. *Aquatic Geochemistry* **9**, 87–110.
- Macur RE, Langner HW, Kocar BD, Inskeep WP (2004a) Linking geochemical processes with microbial community analysis: Successional dynamics in an arsenic-rich, acid-sulfate-chloride geothermal spring. *Geobiology* **2**, 163–177.
- Macur RE, Jackson CR, Botero LM, McDermott TR, Inskeep WP (2004b) Bacterial populations associated with the oxidation and reduction of arsenic in an unsaturated soil. *Environmental Science and Technology* **38**, 104–111.
- Madigan MT, Martinko JM, Parker J (2003) *Brock Biology of Microorganisms*, 10th edn. Prentice Hall, New Jersey.
- Mayer KU, Frind EO, Blowes DW (2002) Multicomponent reactive transport modeling in variably saturated porous media using a generalized formulation for kinetically controlled reactions. *Water Resources Research* **38**, 1174.
- Meng X, Bang S, Korfiatis GP (2000) Effects of silicate, sulfate, and carbonate on arsenic removal by ferric chloride. *Water Research* **34**, 1255–1261.
- Miroshnichenko ML, Rainey FA, Hippe H, Chernyh NA, Kostrička NA, Bonch-Osmolovskaya EA (1998) *Desulfurella kamchatkensis* sp. nov. and *Desulfurella propionica* sp. nov., new sulfur-respiring thermophilic bacteria from Kamchatka thermal environments. *International Journal of Systematic Bacteriology* **48**, 475–479.
- Mukhopadhyay R, Rosen BP, Phung LT, Silver S (2002) Microbial arsenic: from geocycles to genes and enzymes. *FEMS Microbiology Reviews* **26**, 311–325.
- Muller D, Lièvreumont D, Simeonova DD, Hubert JC, Lett MC (2003) Arsenite oxidase *aox* genes from a metal-resistant  $\beta$ -proteobacterium. *Journal of Bacteriology* **185**, 135–141.
- Newman DK, Banfield JF (2002) Geomicrobiology: How molecular-scale interactions underpin biogeochemical systems. *Science* **296**, 1071–1077.
- Nordstrom DK, Ball JW, McCleskey RB (2005) Ground water to surface water: Chemistry of thermal outflows in Yellowstone National Park. In *Geothermal Biology and Geochemistry of Yellowstone National Park* (eds Inskeep WP, McDermott TR). Thermal Biology Institute, Montana State University, Bozeman, Montana, pp. 73–94.
- Nordstrom DK, Southam G (1997) Geomicrobiology of sulfide mineral oxidation. *Reviews in Mineralogy* **35**, 361–390.
- Norris PR, Clark DA, Owen JP, Waterhouse S (1996) Characteristics of *Sulfobacillus acidophilus* sp. nov. and other moderately thermophilic mineral-sulphide-oxidizing bacteria. *Microbiology* **142**, 775–783.
- Oremland RS, Hoelt SE, Santini JM, Bano N, Hollibaugh RA, Hollibaugh JT (2002) Anaerobic oxidation of arsenite in Mono lake water and by a facultative, arsenite-oxidizing chemoautotroph, strain MLHE-1. *Applied and Environmental Microbiology* **68**, 4795–4802.
- Oremland RS, Stolz JF (2003) The ecology of arsenic. *Science* **300**, 939–944.
- Peoples TL, Kelly RM (1995) Bioenergetic response of the extreme thermoacidophile *Metallosphaera sedula* to thermal and nutritional stresses. *Applied and Environmental Microbiology* **61**, 2314–2321.
- Reysenbach A-L, Banta A, Civello S, Daly J, Mitchel K, Lalonde S, Konhauser K, Rodman A, Rusterholtz K, Takacs-Vesbach C (2005) Aquificales in Yellowstone National Park. In *Geothermal Biology and Geochemistry of Yellowstone National Park* (eds Inskeep WP, McDermott TR). Thermal Biology Institute, Montana State University, Bozeman, Montana, pp. 129–142.
- Reysenbach AL, Shock E (2002) Merging genomes with geochemistry in hydrothermal ecosystems. *Science* **296**, 1077–1082.
- Rosen BP (2002) Transport and detoxification systems for transition metals, heavy metals and metalloids in eukaryotic and prokaryotic microbes. *Comparative Biochemistry and Physiology* **133**, 689–693.
- Santini JM, Sly LI, Schnagl RD, Macy JM (2000) A new chemolithoautotrophic arsenite-oxidizing bacterium isolated from a gold mine: Phylogenetic, physiological, and preliminary biochemical studies. *Applied and Environmental Microbiology* **66**, 92–97.
- Santini JM, Sly LI, Wen A, Comrie D, De Wulf-Durand P, Macy JM (2002) New arsenite-oxidizing bacteria isolated from Australian gold mining environments-phylogenetic relationships. *Geomicrobiology Journal* **19**, 67–76.
- Seeger AH, Trincone A, Gahrzt M, Stetter KO (1991) *Stygiolobus azoricus* gen. nov., sp. nov., represents a novel genus of anaerobic, extremely thermoacidophilic archaeobacteria of the order *Sulfolobales*. *International Journal of Systematic Bacteriology* **41**, 495–501.
- Shima S, Suzuki KI (1993) *Hydrogenobacter acidophilus* sp. nov., a thermoacidophilic, aerobic, hydrogen-oxidizing bacterium requiring elemental sulfur for growth. *International Journal of Systematic Bacteriology* **43**, 703–708.
- Shock EL, Holland M, Meyer-Dombard DR, Amend JP (2005) Geochemical sources of energy for microbial metabolism in hydrothermal ecosystems: Obsidian Pool, Yellowstone National Park. In *Geothermal Biology and Geochemistry of Yellowstone National Park* (eds Inskeep WP, McDermott TR). Thermal Biology Institute, Montana State University, Bozeman, Montana, pp. 95–112.
- Silver S, Phung LT (2005) Genes and enzymes involved in bacterial oxidation and reduction of inorganic arsenic. *Applied and Environmental Microbiology* **71**, 599–608.
- Spear JR, Walker JJ, McCollum TM, Pace NR (2005a) Hydrogen and bioenergetics in the Yellowstone geothermal ecosystem. *Proceedings of the National Academy of Sciences, USA* **102**, 2555–2560.
- Spear JR, Walker JJ, Pace NR (2005b) Hydrogen and primary productivity: inference of biogeochemistry from phylogeny in a geothermal ecosystem. In *Geothermal Biology and Geochemistry of Yellowstone National Park* (eds Inskeep WP, McDermott TR). Thermal Biology Institute, Montana State University, Bozeman, Montana, pp. 113–128.
- Stauffer RE, Thompson JM (1984) Arsenic and antimony in geothermal waters of Yellowstone National Park, Wyoming, USA. *Geochimica et Cosmochimica Acta* **48**, 2547–2561.
- Stumm W (1984) Interpretation and measurement of redox intensity in natural waters. *Schweiz Zeitschrift für Hydrologie* **46**, 291–296.
- Stumm W, Morgan JJ (1996) *Aquatic Chemistry: Chemical Equilibria and Rates in Natural Waters*, 3rd edn. John Wiley and Sons, New York.
- To TB, Nordstrom DK, Cunningham KM, Ball JW, McCleskey RB

- (1999) New method for the direct determination of dissolved Fe (III) concentration in acid mine waters. *Environmental Science and Technology* **33**, 807–813.
- Wang Y, Van Cappellen P (1996) A multicomponent reactive transport model of early diagenesis: Application to redox cycling in coastal marine sediments. *Geochimica et Cosmochimica Acta* **60**, 2993–3014.
- Ward DM, Ferris MJ, Nold SC, Bateson MM (1998) A natural view of microbial biodiversity within hot spring cyanobacterial mat communities. *Microbiology and Molecular Biology Reviews* **62**, 1353–1370.
- Wilkie JA, Hering JG (1998) Rapid oxidation of geothermal arsenic (III) in streamwaters of the eastern Sierra Nevada. *Environmental Science and Technology* **32**, 657–662.